Convergence of time-space adaptive algorithms for nonlinear conservation laws

Frédéric Coquel[†*], Marie Postel[†*], and Quang-Huy Tran[‡]

December 12, 2010

Abstract

A family of explicit adaptive algorithms is designed to solve nonlinear scalar 1D conservation laws. Based on the Godunov scheme on a uniform grid, a first strategy uses the multiresolution analysis of the solution to design an adaptive grid which evolves in time according to the time dependent local smoothness. The method is furthermore enhanced by a local time stepping strategy. Both numerical schemes are shown to converge towards the unique entropy solution.

Keywords

conservation laws, entropy solution, local time stepping, multiresolution

1 Introduction

It is well-known that nonlinear conservation laws may develop shock solutions in finite time. Since high order schemes are not applicable in the vicinity of these discontinuities, very fine grids are required to ensure precision. On the other hand, nonlinearity usually implies high computing cost for the flux functions which can make the computing time unpracticably expensive if the very fine grid is used everywhere. These simple remarks motivate the need for adaptivity. Note, however, that our context is quite different from the elliptic problems where AMR techniques based on a posteriori error estimates are standardly used. One crucial point is that the mesh must evolve in time, as the singularities of the solution are transported or created.

Over the past twenty years, Harten's framework [19] for multiresolution in space has been at the root of the development of fully adaptive schemes. Multiresolution methods in this framework rely on a dyadic hierarchy of nested grids. Starting from a numerical scheme designed on the uniform finest grid, the local smoothness of the numerical solution is analyzed at each time-step by performing a wavelet transformation. The size of the details in the multiscale domain is tested against a threshold parameter ε. This allows users to select the local size of the mesh according to the time-dependent local smoothness of the solution. The hyperbolicity of the governing PDEs enables us to predict the displacement of the singularity and therefore to monitor the adaptive grid from one time-step to the

[*]CNRS, UMR 7598, Laboratoire Jacques-Louis Lions, F-75005, Paris, France

[†]UPMC Univ Paris 06, UMR 7598, Laboratoire Jacques-Louis Lions, F-75005, Paris, France

[‡]IFP Énergies nouvelles, Département Mathématiques Appliquées, 1 et 4 avenue de Bois-Préau, 92852 Rueil-Malmaison, France

next one. The resulting adaptive schemes have been designed and analyzed in the scalar case in [6]. In particular, an $O(\varepsilon)$ error estimate with respect to the solution obtained using the numerical scheme on the uniform finest grid has been derived. These spatially adaptive methods have been successfully applied to numerous problems where convection is the prevailing phenomenon, going from compressible Navier-Stokes equations [4, 27, 30] to two-phase flows [2, 8, 25] and shallow-water equations [22].

More recently, they have been further enhanced by Local Time Stepping strategies [7, 14, 26]. The idea dates back to Berger and Oliger's original work [3] and consists in using different time-steps according to the local mesh-size. In a contemporary paper, Osher and Sanders [29] established convergence of monotonous scalar finite-volume schemes on nonuniform grids. The time-step is locally adapted to the grid size but the nonuniform grid is fixed throughout the computation.

In the case of explicit scheme for hyperbolic equations, this is particularly interesting since the time-step must satisfy a CFL stability condition. Indeed, if the same time-step were used everywhere in the domain, then it would have to be controlled by the finest grid-size, which could heavily tamper the computing time performance. On the other hand, using different time-steps for different meshes require to synchronize the solution and generates additional overall costs due to book-keeping. The numerical results are nonetheless very interesting from the computing time and memory savings points of view.

In previous works [1,7,8], we extensively used multiresolution schemes with and without local time stepping strategy on systems of hyperbolic PDEs. In this paper, we propose an analysis of both adaptive schemes in the scalar case. To this end, we follow a proof strategy designed by Coquel and LeFloch [10] which appears to be best-suited to our problem. We show that both schemes converge in the weak sense towards the unique entropy solution of the continuous equation. In the case of the fully adaptive scheme using a global time step, our result is not as powerful as the error estimate obtained by Cohen et al. [6]. Its interest, however, lies in its extension to the local time stepping strategy, where to our knowledge no other convergence results are available.

The paper is outlined as follows. Section 2 starts by recalling the background results for studying weak and measure-valued solutions of conservation laws, then introduces a generic method to prove convergence of approximate sequence of solutions. Section 3 explains the setup of Harten's multiresolution to design our adaptive schemes and provides one of the estimate needed to prove convergence. The adaptive numerical schemes are described and studied in sections 4 and 5.

2 Statement of the problem

2.1 Solution to a scalar conservation law

For $T > 0$, let us consider the Cauchy problem

$$\partial_t u(x,t) + \partial_x f(u(x,t)) = 0, \qquad x \in \mathbb{R}, \quad t \in]0,T[, \tag{2.1a}$$

$$u(x,0) = u_0(x), \qquad x \in \mathbb{R}, \tag{2.1b}$$

where $u : \mathbb{R} \times [0,T] \to \mathbb{R}$ is the unknown function; $f : \mathbb{R} \to \mathbb{R}$ is a given flux function, assumed to be C^1; $u_0 : \mathbb{R} \to \mathbb{R}$ is a given initial data, assumed to be L^∞.

It is well-known [16,17] that problem (2.1) does not have a smooth solution in general, insofar as shocks may appear in finite time. This difficulty regarding existence can be

overcome by introducing weak solutions via distributions. Furthermore, in order to ensure uniqueness, it is necessary to supplement (2.1) with the entropy condition

$$\partial_t \eta(u(x,t)) + \partial_x q(u(x,t)) \leq 0 \tag{2.2}$$

in the sense of distributions for all entropy/entropy-flux pairs (η, q). A pair of real-valued C^1-functions $(\eta, q) : \mathbb{R} \to \mathbb{R} \times \mathbb{R}$ is said to be an entropy/entropy-flux pair if η is convex and if

$$\eta'(u) f'(u) = q'(u), \qquad u \in \mathbb{R}. \tag{2.3}$$

To put it another way, the entropy-decreasing requirement (2.2) for all entropy/entropy-flux pairs allows the physically relevant solution to be singled out among all the possible weak solutions of (2.1) in the scalar case [16, 32]. This solution u obeys

$$\|u\|_{L^\infty(\mathbb{R}\times[0,T])} \leq \|u_0\|_{L^\infty(\mathbb{R})}, \tag{2.4}$$

which means that the range of values taken by u is a.e. included in that of u_0.

2.2 Sequences of approximate solutions

Given a uniform mesh of size Δx and given a time-step Δt, it is customary to approximate the entropy solution u of problem (2.1) by a piecewise-constant function $u_{\Delta x, \Delta t}$, defined as

$$u_{\Delta x, \Delta t}(x,t) = u_j^n, \qquad \text{for } (x,t) \in [x_{j-1/2}, x_{j+1/2}[\times [t^n, t^{n+1}[, \tag{2.5}$$

where $x_{j-1/2} = j\Delta x$ and $t^n = n\Delta t$. The u_j^n's are computed according to the explicit scheme

$$u_j^{n+1} = u_j^n - \frac{\Delta t}{\Delta x}(F(u_j^n, u_{j+1}^n) - F(u_{j-1}^n, u_j^n)) \tag{2.6a}$$

$$u_j^0 = \frac{1}{\Delta x}\int_{x_{j-1/2}}^{x_{j+1/2}} u_0(x)dx. \tag{2.6b}$$

where $F(.,.)$ stands for some numerical flux consistent with f. We refer the reader to [16] for precise definitions and some canonical examples. In what follows, we will be concerned with entropy-satisfying finite-volume methods such that for every entropy/entropy-flux pair (η, q), there holds a discrete entropy inequality of the form

$$\eta(u_j^{n+1}) \leq \eta(u_j^n) - \frac{\Delta t}{\Delta x}(Q(u_j^n, u_{j+1}^n) - Q(u_{j-1}^n, u_j^n)), \tag{2.7}$$

where $Q(.,.)$ is a numerical entropy flux consistent with q (see [16] again). The issue to be examined is the convergence of the time explicit scheme (2.6) under some CFL constraint

$$\frac{\Delta t}{\Delta x}\max_u |f'(u)| < \frac{1}{2}, \tag{2.8}$$

for all u under consideration. That is, the proposer of any scheme of the type (2.6) has to prove that the corresponding family $u_{\Delta x, \Delta t}$ does indeed converge to the entropy solution u when

$$(\Delta x, \Delta t) \to (0,0) \quad \text{with } \frac{\Delta t}{\Delta x} = \text{Cte}. \tag{2.9}$$

In this paper, we shall be concerned with the convergence issue for the approximate solutions $u_{\Delta x,\Delta t,\varepsilon}$ produced by the two classes of adaptive schemes that we previously advocated in [1, 7, 8] for the numerical approximation of (2.1). The first class, based upon Cohen et al. [6], is called *Global Time Stepping* because we have space-only adaptivity and a single time-step is used for all meshes. The second class, partially based upon Müller and Stiriba [26], is called *Local Time Stepping* because we have full space-time adaptivity and each mesh is assigned its own time-step. Besides a reference mesh-size Δx (representing the coarsest level) and a reference time-step Δt (representing the largest time-step), the computed solution also depends on a threshold parameter ε. The latter parameter is homogeneous to an interpolation error and is aimed at monitoring the local coarsening or refining of the grid.

Unlike the uniform grid case, the actual construction of the piecewise-constant function $u_{\Delta x,\Delta t,\varepsilon}$ is quite involved, as will be detailed in §4 and §5. It includes so many technicalities that it is impossible for us at this stage to write down an update formula as simple as (2.6). However, we are in a position to state our purpose, which is to prove that the family $u_{\Delta x,\Delta t,\varepsilon}$ does indeed converge to the entropy solution u of (2.1) when

$$(\Delta x, \Delta t, \varepsilon) \to (0,0,0) \quad \text{with} \quad \frac{\Delta t}{\Delta x} = \text{Cte} \quad \text{and} \quad \frac{\varepsilon}{\Delta t} = \text{Cte}, \tag{2.10}$$

under a CFL restriction similar —but not identical— to (2.8). For notational convenience and thanks to (2.10), we shall henceforth write u_ε instead of $u_{\Delta x,\Delta t,\varepsilon}$. The relation between ε and Δt will be commented upon in paragraph 4.2.1.

2.3 Strategy for a proof of convergence

To achieve this goal, we appeal to the general framework set forth by Coquel and LeFloch [9,10]. This approach was initially proposed to replace traditional BV-oriented techniques [15, 18, 21, 23, 31, 35] in the unfavorable case of sequences of approximate solutions that fail to satisfy a BV-estimate. This occurs for instance in several space dimensions, where BV-estimates are not always available. Even in one space dimension, the assumptions it requires are also weaker than a BV-estimate. For a scalar conservation law in one space dimension, it appears to be one of the fastest way to derive convergence.

In essence, the Coquel-LeFloch method relies on former results by DiPerna [13] regarding uniqueness of measure-valued solutions and consistency with the initial solution (see Appendix A). Although it makes use of entropy inequalities and shares a few common tools with the theory of compensated compactness [11, 12, 24, 28, 34], it differs from compensated compactness in that the latter applies only to one space dimension but can be extended to a system of conservation laws. Finally, let us mention that DiPerna's results have also inspired Szepessy's proof of convergence [33] for the streamline diffusion method.

As elaborated on in [10, §2.3], the Coquel-LeFloch program consists of a five-step procedure, upon the successful completion of which u_ε will be proved to converge to u in a strong L^1_{loc} sense:

1. *Derivation of a uniform L^∞-estimate.* The first task is to work out a uniform estimate of the type

$$\|u_\varepsilon\|_{L^\infty(\mathbb{R}\times]0,T[)} \leq C. \tag{2.11}$$

   Then, according to Tartar's celebrated result [34], we are able to define a Young measure ν that yields all the L^∞ weak-$\star$ composite limits of u_ε when $\varepsilon \to 0$. In

other words, for all continuous functions $a : \mathbb{R} \to \mathbb{R}$, we have

$$a(u_\varepsilon) \to \langle \nu, a \rangle \quad \text{weak-}\star \text{ in } L^\infty(\mathbb{R}\times]0,T[). \tag{2.12}$$

The meaning of $\langle \nu, a \rangle$ can be found in Appendix A.

2. *Weak estimate of the discrete space derivatives.* The second task is to bound the fluctuations of the approximate functions u_ε; this is usually done by some uniform estimate on their discrete derivatives, which is weaker than a BV-estimate. This allows us to infer that the limit ν is a measure-valued solution of (2.1) in the sense of Definition A.1.

3. *Derivation of entropy inequalities.* The third task is to prove that for all entropy-entropy flux pair, there holds an inequality similar to (2.7) in the uniform mesh case, possibly with some additional right-hand side source terms that vanish when $\varepsilon \to 0$. This enables us to show that ν satisfies all the entropy inequalities in the sense of Definition A.2.

4. *Consistency with the initial condition.* The fourth task is to check that ν is consistent with the initial data using a criterion by DiPerna (Theorem A.2). To this end, only one strictly convex entropy is required. Once this has been done, it follows that the Young measure ν assumes the correct initial data.

5. *Application of DiPerna's uniqueness theorem.* The fifth task is to invoke DiPerna's uniqueness theorem [13] (see also Theorem A.1) to conclude that $\nu = \delta_u$ where u is the unique entropy weak solution of (2.1). The convergence of u_ε toward u can then be shown to be strong in L^1_{loc}.

In practice, it turns out that instead of a five-step procedure, we only have to concentrate on a two-item check-list, namely:

– STEP 1 : *Derivation of a uniform L^∞-estimate.*
For an adaptive grid, Step 1 is not as straightforward as for the standard uniform mesh, due to the fact that interpolation on an adaptive mesh does induce small fluctuations in the numerical solutions, thus preventing an invariant region to be easily defined.

– STEP 3 : *Derivation of entropy inequalities.*
It is sufficient to derive the entropy inequalities described in Step 3, because these will in turn help us with Tasks 2, 4 and 5 via some classical arguments [10] that can be repeatedly used.

Another difficulty in applying this program lies in the apparent complexity of the algorithms involved in the construction of the approximate solution u_ε on adaptive grids. We now proceed to explaining the underlying ideas behind such a complexity.

3 Basics of multiresolution analysis

We start by addressing the question of how to associate to a given function v and a given threshold ε an adaptive grid S and an approximate piecewise-constant representation $\mathbf{v}_S$ of v on S within the accuracy ε.

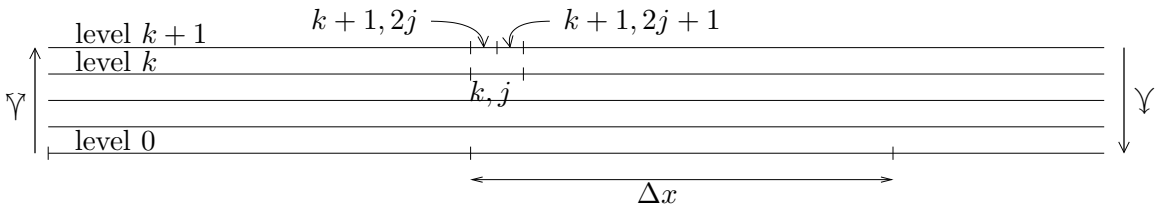

Figure 1: Multiresolution dyadic grid hierarchy, projection and prediction

3.1 Operations on nested uniform grids

We consider a uniform grid with step-size Δx, whose cells are the intervals

$$\Omega_{0,j} = [x_{0,j-1/2}, x_{0,j+1/2}[= [j\Delta x, (j+1)\Delta x[\,, \qquad j \in \mathbb{Z}. \tag{3.1}$$

From this coarsest level labeled 0, we define a hierarchy of grids by dyadic refinement. More specifically, for increasing index $k \geq 0$, the cells of level k are

$$\Omega_{k,j} = [x_{k,j-1/2}, x_{k,j+1/2}[= [2^{-k}j\Delta x, 2^{-k}(j+1)\Delta x[\,, \qquad j \in \mathbb{Z}, \tag{3.2}$$

so that the subdivision property

$$\Omega_{k,j} = \Omega_{k+1,2j} \cup \Omega_{k+1,2j+1} \tag{3.3}$$

holds true and results in a nested hierarchy. The length Δx_k of $\Omega_{k,j}$ is $2^{-k}\Delta x$. The cell-division process stops at the finest level $K \geq 1$.

3.1.1 Coarsening and refining

Let $v : x \in \mathbb{R} \to v(x) \in \mathbb{R}$ be a real-valued function. Initially, v is discretized on the finest grid K by the array $\mathbf{v}_K = \{v_{K,j}\}_{j\in\mathbb{Z}}$ in which $v_{K,j}$ is the average of v over $\Omega_{K,j}$. ¿From this finest level K, we define lower-level representations $\mathbf{v}_k = \{v_{k,j}\}_{j\in\mathbb{Z}}$ of v by successively applying the coarsening operator $\curlyvee$, namely,

$$\mathbf{v}_k = \curlyvee \mathbf{v}_{k+1}, \qquad \text{with} \quad v_{k,j} = \tfrac{1}{2}(v_{k+1,2j} + v_{k+1,2j+1}). \tag{3.4}$$

By nestedness and backward induction, $v_{k,j}$ is the average of v over $\Omega_{k,j}$.

The "inverse" operator attempts to guess the mean values on level $k+1$ from those on level k. This involves a prediction operator $\curlywedge$ which we define as

$$\widehat{\mathbf{v}}_{k+1} = \curlywedge \mathbf{v}_k, \qquad \text{with} \quad \widehat{v}_{k+1,2j+i} = \sum_{m=-s}^{s} \gamma_m^i v_{k,j+m} \ \text{ for } \ i = 0, 1. \tag{3.5}$$

The coefficients γ_m^i are required to meet

$$\gamma_0^0 = 1; \qquad \gamma_0^1 = 1; \tag{3.6a}$$

$$\gamma_m^0 = -\gamma_{-m}^0; \quad \gamma_m^1 = -\gamma_m^0 \qquad \text{for } \ m \neq 0. \tag{3.6b}$$

By construction, these constraints secure (3.4). In other words, the mean values are preserved, and we have $\curlyvee \circ \curlywedge \mathbf{v}_k = \mathbf{v}_k$ for all vector $\mathbf{v}_k$. The prediction operator $\curlywedge$ is local and the width of its stencil is $2s+1$. It is exact for polynomials of degree lesser than $2s$, which means that if v is such a polynomial and if $v_{k+1,j}$ is the average of v over $\Omega_{k+1,j}$ for all $j \in \mathbb{Z}$, then $\curlywedge \circ \curlyvee \mathbf{v}_{k+1} = \mathbf{v}_{k+1}$.

3.1.2 Encoding and decoding

The detail $\mathbf{d}_{k+1} = \{d_{k+1,j}\}_{j\in\mathbb{Z}}$ is defined to be the array whose entries are

$$d_{k+1,j} = v_{k+1,j} - \widehat{v}_{k+1,j}. \tag{3.7}$$

Since the preservation of mean values implies

$$v_{k+1,2j} = \widehat{v}_{k+1,2j} + d_{k+1,2j} \tag{3.8a}$$

$$v_{k+1,2j+1} = \widehat{v}_{k+1,2j+1} - d_{k+1,2j}, \tag{3.8b}$$

or in other words

$$d_{k+1,2j+1} = -d_{k+1,2j}. \tag{3.9}$$

Because $\widehat{\mathbf{v}}_{k+1} = \curlyvee \mathbf{v}_k$, the pair $(\mathbf{v}_k, \mathbf{d}_{k+1})$ can be stored in place of $\mathbf{v}_{k+1}$ without any loss of information, and using (3.9) with the same storage space. Iterating this process from the finest level down to the coarsest yields the $(K+1)$-tuple $(\mathbf{v}_0, \mathbf{d}_1, \ldots, \mathbf{d}_K)$, which we refer to as the multiscale representation of $\mathbf{v}_K$. For convenience, we set $\mathbf{d}_0 = \mathbf{v}_0$ and formally express this as

$$\mathbf{m} = (\mathbf{d}_0, \mathbf{d}_1, \ldots, \mathbf{d}_K) = \mathtt{M}\mathbf{v}_K, \tag{3.10}$$

where $\mathtt{M}$ denotes the encoding operator.

The inverse operator $\mathtt{M}^{-1}$ acts on the multiscale representation $\mathbf{m}$ and returns the arrays $\mathbf{v}_k$ for $0 \le k \le K$ using the two-scale relations (3.8) and the prediction operator (3.5). It is said to be the decoding operator.

3.1.3 Thresholding and approximating

By virtue of the polynomial exactness of the prediction operator (3.5), a detail that is small in absolute value implies that the function v is locally "close" to a polynomial. We take advantage of this property to compress the function in the multiscale domain by dropping the details that are smaller than a given threshold.

To clarify this idea, we first define a threshold operator $\mathtt{T}_\Gamma$ depending on an arbitrary subset $\Gamma \subset \{0, 1, \ldots, K\} \times \mathbb{Z}$ of indices (k, j). Let $\mathbf{m} = (\mathbf{d}_0, \mathbf{d}_1, \ldots, \mathbf{d}_K)$ be a multiscale representation. Then, we set

$$\mathtt{T}_\Gamma \mathbf{m} = (\mathbf{d}_0', \mathbf{d}_1', \ldots, \mathbf{d}_K') \tag{3.11}$$

where

$$d_{k,j}' = \begin{cases} d_{k,j} & \text{if } (k,j) \in \Gamma, \\ 0 & \text{otherwise.} \end{cases} \tag{3.12}$$

The operator $\mathtt{T}_\Gamma$ amounts to cancelling all the components of a multiscale representation lying outside Γ.

Given a threshold $\varepsilon > 0$, we introduce the level-dependent threshold values

$$\varepsilon_0 = 0 \qquad \text{and} \qquad \varepsilon_k = 2^{k-K}\varepsilon \quad \text{for } k = 1, \ldots, K. \tag{3.13}$$

The rationale for (3.13) is that the coarser a level is, the more cautious we must be in dropping out details. Then, the subsets Γ of interest to us are those which contain the region of *significant* details, that is,

$$\Gamma \supset \Gamma_\varepsilon := \{(k,j) \in \{0, 1, \ldots, K\} \times \mathbb{Z} \text{ such that } |d_{k,j}| \ge \varepsilon_k\} \tag{3.14}$$

and which are a *gradual*, that is,

$$(k+1,j) \in \Gamma \Rightarrow (k, \lfloor j/2 \rfloor + \ell) \in \Gamma, \quad \text{for } \ell = -g, \dots, g. \tag{3.15}$$

To turn any subset Γ into a gradual tree, we use Algorithm 1. Choosing the grading parameter $g \geq s$ ensures that the stencil of the predictive refining operator (3.5) always belongs to the tree. Applying Algorithm 1 to Γ_ε yields the smallest acceptable tree, which we also designate by Γ_ε.

Algorithm 1 Gradualness of the tree

```
for level k = K − 1 ↘ 0 do
  for j ∈ ℤ do
    if (k + 1, j) ∈ Γ then
      ensure that (k, ⌊j/2⌋ + ℓ) ∈ Γ for all ℓ = −g, ..., g.
    end if
  end for
end for
```

From the thresholding operator $\mathtt{T}_\Gamma$, introduced in (3.11)–(3.12), we define the approximating operator

$$\mathtt{A}_\Gamma = \mathtt{M}^{-1}\mathtt{T}_\Gamma\mathtt{M} \tag{3.16}$$

which is meant to act on the physical representation $\mathbf{v}_K$. The latter operator is nonlinear, since Γ now depends on $\mathbf{v}_K$ through (3.14). It reveals itself to be a "good" approximation, in the sense that we have the two estimates

$$\|\mathbf{v}_K - \mathtt{A}_\Gamma \mathbf{v}_K\|_{L^1} \leq C_1 \varepsilon, \tag{3.17a}$$

$$\|\mathbf{v}_K - \mathtt{A}_\Gamma \mathbf{v}_K\|_{L^\infty} \leq C_\infty \varepsilon, \tag{3.17b}$$

where the constants C depend on the prediction operator (3.5)–(3.6) and provided that

$$\|\mathbf{v}_K\|_{L^1} = \Delta x_K \sum_{j\in\mathbb{Z}} |v_{K,j}| \qquad \text{and} \qquad \|\mathbf{v}_K\|_{L^\infty} = \sup_{j\in\mathbb{Z}} |v_{K,j}| \tag{3.18}$$

are well-defined. We refer the readers to Cohen [5] for the proof and also for a thorough investigation of nonlinear approximation.

3.2 Operations on adaptive non-uniform grids

3.2.1 From a tree to a grid

For a significant and gradual tree Γ satisfying (3.14)–(3.15), we consider the set

$$\partial\Gamma = \big\{(k,j) \text{ such that } (k, 2\lfloor j/2 \rfloor) \in \Gamma \text{ and } (k+1, 2j) \notin \Gamma\big\}, \tag{3.19}$$

representing its leaves[1], where the finest non-negligible detail is located. Thus, (k,j) belongs to $\partial\Gamma$ if its parent $(k-1, \lfloor j/2 \rfloor)$ is too coarse ($|d_{k,2\lfloor j/2 \rfloor}| \geq \varepsilon_k$) and if it is itself fine enough to render the local smoothness of the solution ($|d_{k+1,2j}| < \varepsilon_{k+1}$). Let

$$S = S(\Gamma) := \{\Omega_{k,j}\}_{(k,j)\in\partial\Gamma} \tag{3.20}$$

[1]For $k = K$, it is conventionally understood that $(K+1, j) \notin \Gamma$

be the collection of cells in the x-domain corresponding to the pairs (k,j) in $\partial\Gamma$. To emphasize that S depends on Γ, we may be led to write $S(\Gamma)$. It must be kept in mind that while $\partial\Gamma$ is merely a set of integer pairs (k,j), the associated grid S is a collection of intervals of the x-domain $\mathbb{R}$. It can be readily shown that S induces a partition of this domain, i.e.,

$$\mathbb{R} = \bigcup_{(k,j)\in\partial\Gamma} \Omega_{k,j} \tag{3.21}$$

and $\Omega_{k,j} \cap \Omega_{k',j'} = \emptyset$ for $(k,j) \neq (k',j')$. It follows that S can also be considered as a (non-uniform) space grid. For $\Omega_{k,j} \in S$, the left (resp. right) neighbor of $\Omega_{k,j} \in S$ is designated by Ω_{k_L,j_L} (resp. Ω_{k_R,j_R}). By gradualness of Γ, we have $|k_L - k| \leq 1$ and $|k_R - k| \leq 1$, thus avoiding abrupt level transitions. Naturally, it is expected that the higher-level cells of S will be concentrated only around the singularities of v. From now on, the index set $\partial\Gamma$ of the adaptive grid S will also be referred to as $\eth S$.

The estimates (3.17) give us strong indication that the tree Γ, and therefore the grid S, are well suited to the data $\mathbf{v}_K$ within an accuracy defined by ε. In assessing the effects of thresholding by (3.17), however, we have used $\mathtt{A}_\Gamma \mathbf{v}_K = \mathtt{M}^{-1}(\mathtt{T}_\Gamma \mathtt{M} \mathbf{v}_K)$, a vector defined on level K. While this vector is convenient for such a theoretical purpose, what is really needed for practical computations is a representation of v on the adaptive grid S. This representation $\mathbf{v}_S = \{v_{k,j}\}_{(k,j)\in\eth S}$ would consist of approximate average values of v over each $\Omega_{k,j} \in S$. We can retrieve it by $\mathbf{v}_S = \mathtt{M}_S^{-1}(\mathtt{T}_\Gamma \mathtt{M} \mathbf{v}_K) = \mathtt{M}_S^{-1} \mathbf{m}_\Gamma$, where $\mathtt{M}_S^{-1}$ is given by the partial decoding Algorithm 2. It can be checked that thanks to gradualness of Γ and to $g \geq s$, Algorithm 2 is well-defined.

Algorithm 2 Partial decoding

Starting from $\mathbf{m}_\Gamma = \mathtt{T}_\Gamma \mathtt{M} \mathbf{v}_K$ on Γ
for level $k = 1 \nearrow K$ **do**
  for $j \in \mathbb{Z}$ **do**
    if $(k,j) \in \Gamma$ **then**
      compute $\begin{cases} \widehat{v}_{k,2j} \text{ using (3.5)}, \\ v_{k,2j} = \widehat{v}_{k,2j} + d_{k,2j}, \\ v_{k,2j+1} = 2v_{k-1,j} - v_{k,2j}. \end{cases}$
    end if
  end for
end for

The reverse transformation $\mathtt{M}_S$ maps $\mathbf{v}_S$ to $\mathbf{m}_\Gamma$ and is performed with the partial encoding Algorithm 3. This time, the algorithm can be checked to be well-defined thanks not only to gradualness and $g \geq s$, but also to the data $v_{k,j}$ available for $(k,j) \in \partial\Gamma$. By construction, the entries of the multiscale representation $\mathtt{M}_S \mathbf{v}_S = (\mathbf{v}_0, \mathbf{d}_1, \ldots, \mathbf{d}_K)$ obtained are equal to zero as soon as $(k,j) \notin \Gamma$.

Remark 3.1. For a finite domain of length $L = N_0 \Delta x$, the grading property imposed by Algorithm 1 ensures that the complexity of the partial decoding and encoding Algorithms 2 and 3 is reduced to $O(\#\Gamma)$ instead of $O(2^K)$.

Algorithm 3 Partial encoding

Starting from $\mathbf{v}_S$ on S
Set $d_{k,j} = 0$ for all (k, j) initially
for level $k = K - 1 \searrow 0$ **do**
  for $j \in \mathbb{Z}$ **do**
    if $(k + 1, 2j) \in \Gamma$ **then**
      compute $v_{k,j}$ using (3.4)
    end if
  end for
  for $j \in \mathbb{Z}$ **do**
    if $(k + 1, j) \in \Gamma$ **then**
      compute $d_{k+1,2j} = v_{k+1,2j} - \widehat{v}_{k+1,2j}$ using (3.5).
    end if
  end for
end for

4 Global Time Stepping adaptive scheme

4.1 Description of the numerical scheme

We now recall how the multiresolution analysis is coupled with the finite-volume approach to design an adaptive method to solve (2.1). The details and the error analysis of the method in the scalar case can be found in [6]. The idea is to represent the solution v_ε^n at a given time step t^n on an adaptive grid $\widetilde{S}_\varepsilon^{n+1}$ suitable for both the current time step and the next one. The design of $\widetilde{S}_\varepsilon^{n+1}$ will be detailed below. The solution is updated using a numerical scheme designed to solve the PDE (2.1) on a non uniform grid. It is then encoded again in the multiresolution representation, in order to update the adaptive grid, according to the displacement and formation of the singularities.

Starting from an initial condition defined as

$$v_{k,j}^0 = \frac{1}{|\Omega_{k,j}|} \int_{\Omega_{k,j}} u_0(x)dx, \qquad \text{for } (k, j) \in \partial\Gamma^0, \tag{4.1}$$

the multiresolution scheme can be summarized as follows:

Algorithm 4 Adaptive algorithm

Initialization: encoding of the initial solution defined by (4.1) and definition of Γ_ε^0 using (3.14).
for time step $n = 0, \ldots, N - 1$ **do**
  Prediction of $\widetilde{\Gamma}_\varepsilon^{n+1}$ using Algorithm 5
  Partial decoding of v^n on $\widetilde{S}_\varepsilon^{n+1}$ (derived from $\widetilde{\Gamma}_\varepsilon^{n+1}$ using (3.20)).
  Evolution of v^n to v^{n+1} on the adaptive grid $\widetilde{S}_\varepsilon^{n+1}$
  Definition of Γ_ε^{n+1} by partial encoding of v^{n+1} and thresholding.
end for
Decoding of v^N on the finest grid S_K.

The stability of the method has been established by a bound on the error between the numerical solution u_ε obtained with Algorithm 4 reconstructed on the finest level S_K in

the grid hierarchy and the numerical solution u obtained with the underlying finite volume scheme on this fine uniform grid. The error estimate

$$\|{u_\varepsilon}^N - u^N\| \leq C(T)\varepsilon \tag{4.2}$$

was obtained for first-order finite-volume schemes by Cohen et al. [6]. It was later extended by Hovhannisyan and Müller [20] to schemes using approximate fluxes and source reconstruction strategies. In the present paper, we are concerned with the convergence of the numerical solution provided by Algorithm 4 towards the entropic solution in the sense defined in paragraph 2.2. We will endeavour to obtain this convergence in a way which can then be extended to the local time stepping strategy.

The prediction of the tree $\widetilde{\Gamma}_\varepsilon^{n+1}$ is actually the bottleneck of the method. Thanks to the hyperbolicity of the system of PDEs, the singularities move at finite speed. The CFL stability condition (2.8) enables us to predict their propagation and also their formation during one time step. It was shown in [6] that it is actually possible to design a grid suitable to represent the solution at two consecutive times steps t^n and t^{n+1}. To this extent, the size of each significant detail $d_{k,j}^n$ is tested against the threshold parameter ε_k to determine a unique index $p(k,j)$ such that

$$2^{p(k,j)z}\varepsilon_k \leq |d_{k,j}^n| \leq 2^{(p(k,j)+1)z}\varepsilon_k. \tag{4.3}$$

In the above inequalities, z is a real number such that $z < r+1$, with r the C^r-Hölder smoothness of the wavelet which underlies the reconstruction scheme. In our case $r < 1$, therefore $z < 2$. The index $p(k,j)$ is the number of levels to be refined starting from k, in a way which preserves the grading of the initial tree. To make this precise, let us recall some definitions from [6]:

- the *range of influence* of a detail $d_{k,j}$ contains the indexes of the cells at the finest level that depend on the detail

$$\Sigma_{k,j} = \{2^{K-k}(j-2s) + 2s, \ldots, 2^{K-k}(j+2s+1) - 2s - 1\}; \tag{4.4}$$

- the *set of dependance* of a detail $d_{k,j}$ contains the indexes of the cells at the finest level which the detail depends on

$$\widetilde{\Sigma}_{k,j} = \{2^{K-k}(j-s), \ldots, 2^{K-k}(j+s+1) - 1\}; \tag{4.5}$$

- the evolution during one time step with a q-stencil finite volume scheme is taken into account by defining the *backward dependance set*

$$\widetilde{\Sigma}_{k,j}^- = \bigcup_{m \in \widetilde{\Sigma}_{k,j}} \{m-q, \ldots, m+q\}. \tag{4.6}$$

The refinement of the tree Γ_ε^n is then performed according to the following algorithm:

The grid $\widetilde{S}_\varepsilon^{n+1} = S(\widetilde{\Gamma}_\varepsilon^{n+1})$ is a collection of cells $(\Omega_{k,j})_{k,j}$ on different levels k, with the double indices $(k,j) \in \partial\widetilde{\Gamma}_\varepsilon^{n+1}$ defined by (3.19). It is another partition of the domain $\Omega = \cup_l \Omega_{0,l}$. Note that in practice the solution is decoded on $\widetilde{S}_\varepsilon^{n+1}$ only in order to be updated with the finite-volume scheme. Nevertheless, in order to analyze the convergence of the method, we introduce operators who perform the different steps of the Algorithm

Algorithm 5 Prediction of the adaptive tree $\widetilde{\Gamma}_\varepsilon^{n+1}$

Require: The solution is thresholded in the multiscale representation (3.10) on the partial tree Γ_ε^n defined by (3.14).
for level $k = K-1 \searrow 1$ **do**
  if $(k,j) \in \Gamma_\varepsilon^n$ **then**
    find $p(k,j)$ with (4.3)
    add to $\widetilde{\Gamma}_\varepsilon^{n+1}$ all (k',j') such that $k' \leq k + p(k,j)$ and $\widetilde{\Sigma}^-_{k',j'} \cap \Sigma_{k,j} \neq \emptyset$.
  end if
end for
Apply grading Algorithm 1 to $\widetilde{\Gamma}_\varepsilon^{n+1}$.

4 on the solution in the physical domain. The action of these operators on a Riemann problem for one time-step is illustrated in Figure 2.

Since the evolution scheme is explicit in time, the time step must satisfy a CFL stability condition. The grid being non-uniform, condition (2.8) is replaced by

$$\frac{\Delta t}{2^K \Delta x} \max_u |f'(u)| < \frac{1}{2}. \tag{4.7}$$

Note that it is much more severe than the uniform case condition, since it makes the time step of the same order than the smallest space step. This is a major incitement to design a scheme where different time-steps are used according to the local space discretization. This will be the subject of section 5.

Let us now focus on the various operators involved in one time-step for the Global Time Stepping adaptive scheme.

- Operator `E` (Evolution): this corresponds to the first step of the standard Godunov scheme under CFL condition (4.7). It computes the solution of the Cauchy problem

$$\partial_t u_\varepsilon(x,t) + \partial_x f(u_\varepsilon(x,t)) = 0, \qquad x \in \mathbb{R}, \qquad t \in [t^n, t^{n+1}[, \tag{4.8a}$$

$$u_\varepsilon(x,t^n) = v^n_{k,j}, \qquad x \in \Omega_{k,j}, \quad (k,j) \in \partial\widetilde{\Gamma}_\varepsilon^{n+1}. \tag{4.8b}$$

  on the time interval $[t^n, t^{n+1}[$. We use the notation

$$\mathtt{E}u_\varepsilon(x,t^n) = u_\varepsilon(x,t^{n+1,-}) \tag{4.9}$$

  to express the limit of u_ε as $t \to t^{n+1}$ from lower values.

- Operator `P` (Projection): this corresponds to the second step of the Godunov scheme. It computes the average of the Cauchy problem solution on the cells of the grid $\widetilde{S}_\varepsilon^{n+1}$. We denote by $\bar{v}^{n+1}_{k,j}$ the discrete values such that

$$\mathtt{P}u_\varepsilon(x,t^{n+1,-}) = \bar{v}^{n+1}_{k,j}, \qquad \text{for } x \in \Omega_{k,j}, \quad (k,j) \in \partial\widetilde{\Gamma}_\varepsilon^{n+1}. \tag{4.10}$$

  Note that combining operators `E` and `P` leads to the numerical scheme

$$\bar{v}^{n+1}_{k,j} = v^n_{k,j} - \frac{\Delta t}{\Delta x_k}\left(f^n_{k_r,j_r} - f^n_{k,j}\right), \tag{4.11}$$

  with

$$f^n_{k_r,j_r} = F(v^n_{k,j}, v^n_{k_r,j_r}), \tag{4.12a}$$

$$f^n_{k,j} = F(v^n_{k_l,j_l}, v^n_{k,j}), \tag{4.12b}$$

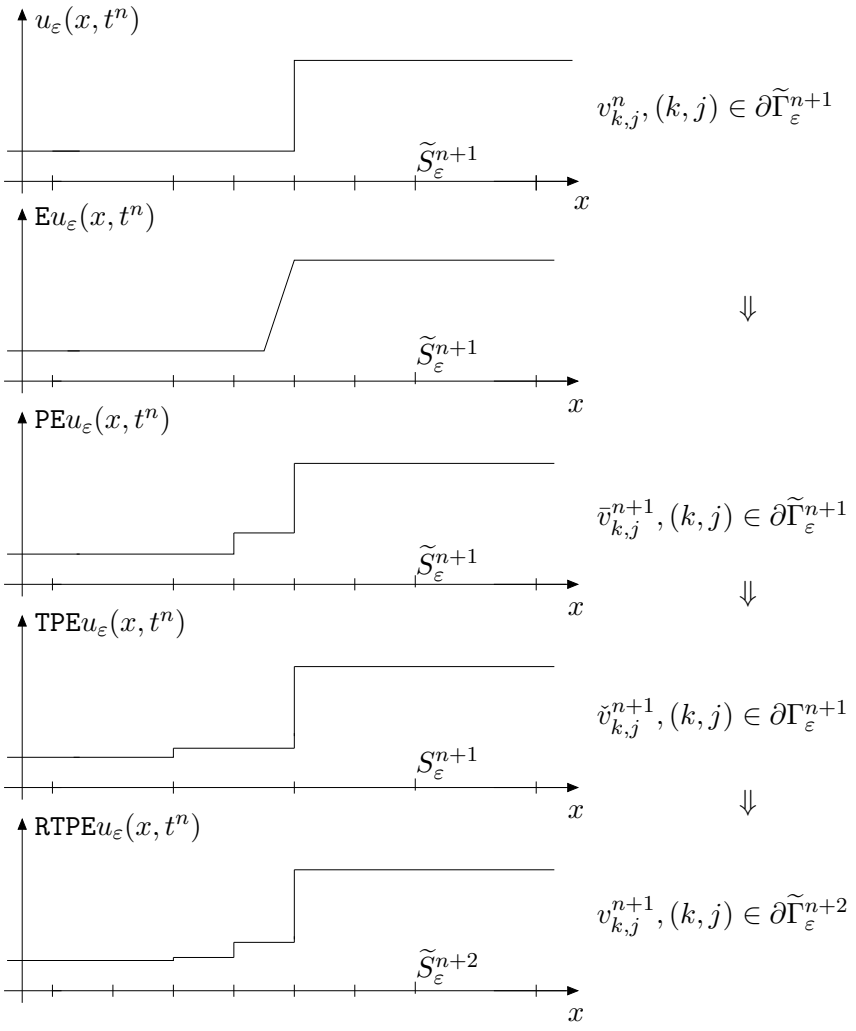

Figure 2: Action of the operators on a Riemann problem for one time-step

and $\Delta t/\Delta x_k$ should satisfy the CFL condition (4.7). The cell Ω_{k_l,j_l} (respectively Ω_{k_r,j_r}) is the left (resp. right) hand side neighbor of cell $\Omega_{k,j}$. In (4.12), F stands for the Godunov numerical flux function

$$F(v_1,v_2)=f(\omega(0^+,v_1,v_2)), \tag{4.13}$$

where $\omega(x/t,v_1,v_2)$ is the self-similar solution of the Riemann problem (2.1) with $u_0(x)=v_1$ for $x<0$ and $u_0(x)=v_2$ for $x\geq 0$. We use the symbol $f_{k,j}$ instead of $f_{k,j-1/2}$ the flux for the left interface of cell $\Omega_{k,j}$ because this notation is more suitable to the multiresolution analysis.

- Operator `T` (Thresholding): apply the multiresolution thresholding which coarsens the solution on the grid $S^{n+1}_\varepsilon=S(\Gamma^{n+1}_\varepsilon)$. We denote by $\check{v}^{n+1}_{k,j}$ the discrete values such that

$$\mathtt{T}\mathtt{P}u_\varepsilon(x,t^{n+1,-})=\check{v}^{n+1}_{k,j},\qquad \text{for } x\in\Omega_{k,j},\ \ (k,j)\in\partial\Gamma^{n+1}_\varepsilon. \tag{4.14}$$

Note that this operator has the same effect on the solution as the projection operator `P` but on a coarser grid. The tools to handle them in the proofs will be the same.

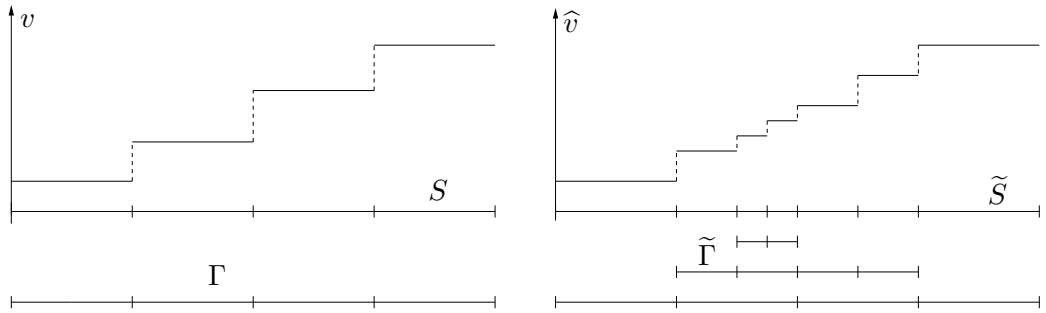

Figure 3: Trees Γ and $\widetilde{\Gamma} \supset \Gamma$, grids $S = S(\Gamma)$ and $\widetilde{S} = S(\widetilde{\Gamma})$, discrete solutions v and $\widehat{v}$

- Operator `R` (Refinement): predicts the tree $\widetilde{\Gamma}_\varepsilon^{n+2}$ containing both Γ_ε^{n+1} and Γ_ε^{n+2} using Algorithm 5. Set to 0 the details $d_{k,j}$ for $(k,j) \in \Gamma_\varepsilon^{n+2}$ and $(k,j) \notin \Gamma_\varepsilon^{n+1}$. Refines the solution from S_ε^{n+1} to $\widetilde{S}_\varepsilon^{n+2} = S(\widetilde{\Gamma}_\varepsilon^{n+2})$ using the partial refinement Algorithm 2. We are back to the discrete values on the predicted grid $\widetilde{S}_\varepsilon^{n+2}$ such that
$$\mathtt{RTP} u_\varepsilon(x, t^{n+1,-}) = v_{k,j}^{\varepsilon,n+1}, \qquad \text{for } x \in \Omega_{k,j},\ (k,j) \in \partial\widetilde{\Gamma}_\varepsilon^{n+2}. \tag{4.15}$$

For each step, we have introduced a notation for the constant solution on the relevant grid along with the operator. This will be useful in the proofs.

In order to control the effect of the refinement operators we first state a technical result due to Cohen et al. [6]. We recall it here in a restricted version which is sufficient for our problem. The underlying idea is that if a detail is negligible, the differences between values on the finest level belonging to its set of dependance defined by (4.5) should also be small.

Lemma 4.1. *Let $(k,j) \notin \widetilde{\Gamma}$, let $m = 2^{K-k}j + \mu$ with $\mu = 0, \dots, 2^{K-k} - 1$ such that*
$$\{m, \dots, m + 2^{K-k} - 1\} \subset \widetilde{\Sigma}_{k,j}^-. \tag{4.16}$$
We designate by $\Delta_L^- v_{k,m} = v_{k,m} - v_{k,m+L}$ the backward differences of gap L on level k. Then, on the finest level K, we have
$$|\Delta_{2^{K-k}}^- v_{K,m}| \le \widetilde{C}\varepsilon_k, \tag{4.17}$$
where the constant $\widetilde{C}$ is uniform and depends only on the underlying wavelet coefficients.

Proof. See [6, Lemma 4.8]. □

Equipped with this result we turn, to the task of bounding the difference between the averages of the solution on cells belonging to the grid S_ε and those on the subdivisions of this cell, belonging to the refined grid $\widetilde{S}_\varepsilon$ (see Figure 3). Since the details on cells belonging to the grid S_ε are negligible by definition (3.20), the values on $\widetilde{S}_\varepsilon$ are obtained using the prediction scheme (3.5).

Lemma 4.2. Effect of the refinement of the tree. *For a given discrete function v, denote by Γ_ε the tree constructed by (3.14) and the grading Algorithm 1 and by $\widetilde{\Gamma}_\varepsilon$ the more refined gradual tree obtained with Algorithm 5 with a grading $g \ge s$. Let S_ε and $\widetilde{S}_\varepsilon$ be the corresponding adaptive grids defined by (3.20). We denote by v the original function reconstructed on S_ε and by $\widehat{v}$ the function reconstructed on $\widetilde{S}_\varepsilon$, after setting to*

zero all details $\mathbf{d}_\lambda$ *such that* $\lambda \in \widetilde{\Gamma}_\varepsilon \backslash \Gamma_\varepsilon$. *Then, for any* $(k,j) \in \partial\Gamma_\varepsilon$ *and any* (p,ℓ) *with* $\ell = 0, \dots 2^p - 1$ *such that* $(k+p, 2^p j + \ell) \in \partial\widetilde{\Gamma}_\varepsilon$, *we have*

$$|\widehat{v}_{k+p,2^p j+\ell} - v_{k,j}| \leq \widetilde{C}\varepsilon_k. \tag{4.18}$$

Proof. First, consider the largest q such that $(k+q, 2^q j + m') \in \partial\widetilde{\Gamma}_\varepsilon$, with $m' = 0, \dots 2^q - 1$. This implies, in particular, that for $p' = q+1$

$$(k+p', 2^{p'} j + \ell') \notin \widetilde{\Gamma}_\varepsilon \qquad \text{for all } \ell' = 0, \dots, 2^{p'} - 1. \tag{4.19}$$

We will then show that

$$|\widehat{v}_{k+p',2^{p'} j+\ell'} - v_{k,j}| \leq \widetilde{C}\varepsilon_k \qquad \text{for all } \ell' = 0, \dots 2^{p'} - 1. \tag{4.20}$$

To do this, rewrite the difference in (4.20) as

$$\widehat{v}_{k+p',2^{p'} j+\ell'} - v_{k,j} = \widehat{v}_{k+p',2^{p'} j+\ell'} - 2^{-p'} \sum_{m=0}^{2^{p'}-1} \widehat{v}_{k+p',2^{p'} j+m} \tag{4.21a}$$

$$= 2^{-p'} \sum_{m=0}^{2^{p'}-1} (\widehat{v}_{k+p',2^{p'} j+\ell'} - \widehat{v}_{k+p',2^{p'} j+m}). \tag{4.21b}$$

The first line (4.21a) holds true thanks to the preservation of the mean value in the reconstruction process. We now split the last sum (4.21b) into two smaller sums. In each of these, we express the summand as a telescoping sum. This yields

$$\sum_{m=0}^{\ell'-1} \sum_{n=m}^{\ell'-1} (\widehat{v}_{k+p',2^{p'} j+n+1} - \widehat{v}_{k+p',2^{p'} j+n}) + \sum_{m=\ell'}^{2^{p'}-1} \sum_{n=\ell'}^{m-1} (\widehat{v}_{k+p',2^{p'} j+n} - \widehat{v}_{k+p',2^{p'} j+n+1}) \tag{4.22}$$

for the value of $2^{p'}(\widehat{v}_{k+p',2^{p'} j+\ell'} - v_{k,j})$. By linear recombination of the differences between consecutive values, we can obviously put $\widehat{v}_{k+p',2^{p'} j+\ell'} - v_{k,j}$ under the form

$$\begin{aligned} \widehat{v}_{k+p',2^{p'} j+\ell'} - v_{k,j} &= 2^{-p'} \sum_{m=0}^{2^{p'}-2} c_{\ell',m} (\widehat{v}_{k+p',2^{p'} j+m} - \widehat{v}_{k+p',2^{p'} j+m+1}) \\ &= 2^{-p'} \sum_{m=0}^{2^{p'}-2} c_{\ell',m} \Delta_1^- \widehat{v}_{k+p',2^{p'} j+m}, \end{aligned} \tag{4.23}$$

where the coefficients $c_{\ell',m}$ are clearly bounded by $|c_{\ell',m}| \leq 2^{p'}$. The next step is to involve values on the finest level K into each difference $\Delta_1^- \widehat{v}_{k+p',2^{p'} j+m}$. Starting from

$$\begin{aligned} \Delta_1^- \widehat{v}_{k+p',2^{p'} j+m} &= \widehat{v}_{k+p',2^{p'} j+m} - \widehat{v}_{k+p',2^{p'} j+m+1} \\ &= \tfrac{1}{2}(\widehat{v}_{k+p'+1,2^{p'+1} j+2m} + \widehat{v}_{k+p'+1,2^{p'+1} j+2m+1} \\ &\qquad - \widehat{v}_{k+p'+1,2^{p'+1} j+2m+2} - \widehat{v}_{k+p'+1,2^{p'+1} j+2m+3}) \\ &= \tfrac{1}{2}(\Delta_2^- \widehat{v}_{k+p'+1,2^{p'+1} j+2m} + \Delta_2^- \widehat{v}_{k+p'+1,2^{p'+1} j+2m+1}) \end{aligned} \tag{4.24}$$

and carrying on by induction, we end up with

$$\Delta_1^- \widehat{v}_{k+p',2^{p'}j+m} = 2^{k+p'-K} \sum_{n=0}^{2^{K-k-p'}-1} \Delta^-_{2^{K-k-p'}} \widehat{v}_{K,2^{K-k-p'}(2^{p'}j+m)+n}. \tag{4.25}$$

We claim that for any $n = 0, \dots, 2^{K-k-p'} - 1$ and any $m = 0, \dots, 2^{p'} - 2$, there exists an integer ℓ between 0 and $2^{p'} - 1$ such that

$$\{2^{K-k-p'}(2^{p'}j + m) + n), \dots, 2^{K-k-p'}(2^{p'}j + m + 1) + n\} \subset \widetilde{\Sigma}_{k+p',2^{p'}j+\ell}, \tag{4.26}$$

where —as introduced in (4.5)—

$$\widetilde{\Sigma}_{k+p',2^{p'}j+\ell} = \{2^{K-k-p'}(2^{p'}j + \ell - s), \dots, 2^{K-k-p'}(2^{p'}j + \ell + s + 1) - 1\} \tag{4.27}$$

is the domain of dependence of a detail on the $k + p'$ level. Indeed, this amounts to saying that

$$2^{K-k-p'}(2^{p'}j + m) + n \geq 2^{K-k-p'}(2^{p'}j + \ell - s), \tag{4.28a}$$

$$2^{K-k-p'}(2^{p'}j + m + 1) + n \leq 2^{K-k-p'}(2^{p'}j + \ell + s + 1) - 1. \tag{4.28b}$$

It is easy to check that inequalities (4.28) are met for $\ell = m+1$ since $s \geq 1$. By definitions (4.5)–(4.6), we have $\widetilde{\Sigma}_{k+p',2^{p'}j+\ell} \subset \widetilde{\Sigma}^-_{k+p',2^{p'}j+\ell}$, and therefore

$$\{2^{K-k-p'}(2^{p'}j + m) + n), \dots, 2^{K-k-p'}(2^{p'}j + m + 1) + n\} \subset \widetilde{\Sigma}^-_{k+p',2^{p'}j+\ell}. \tag{4.29}$$

Properties (4.19) and (4.29) make it possible for us to apply Lemma 4.1 to all of the differences

$$\Delta^-_{2^{K-k-p'}} \widehat{v}_{K,2^{K-k-p'}(2^{p'}j+m)+n}.$$

We thus obtain

$$|\Delta_1^- \widehat{v}_{k+p',2^{p'}j+m}| \leq \widetilde{C}\varepsilon_{k+p'}, \tag{4.30}$$

the constant $\widetilde{C}$ being that of Lemma 4.1. It follows from the decomposition (4.23) that

$$|\widehat{v}_{k+p',2^{p'}j+\ell'} - v_{k,j}| \leq 2^{p'}\widetilde{C}\varepsilon_{k+p'} = \widetilde{C}\varepsilon_k \tag{4.31}$$

from which we obtain

$$|\widehat{v}_{k+q,2^q j+\ell'} - v_{k,j}| = 2^{-1}|(\widehat{v}_{k+p',2(2^q j+\ell)} - v_{k,j}) + (\widehat{v}_{k+p',2(2^q j+\ell)+1} - v_{k,j})| \leq \widetilde{C}\varepsilon_k. \tag{4.32}$$

If $p < q$, we expand again $\widehat{v}_{k+p,2^p j+\ell}$ on level $k + q$ as

$$\widehat{v}_{k+p,2^p j+\ell} - v_{k,j} = 2^{p-q} \sum_{m=0}^{2^{q-p}-1} (\widehat{v}_{k+q,2^{q-p}(2^p j+\ell)+m} - v_{k,j}), \tag{4.33}$$

and by a straightforward majorization, we obtain the sought after result (4.18). □

As a consequence of this estimate, we can bound the L^∞-norm of the difference between the thresholded and the refined solutions. The result stated in the following Proposition will be very useful in the sequel.

Proposition 4.1. *We have*

$$\|\texttt{RTPE}u_\varepsilon(.,t^n) - \texttt{TPE}u_\varepsilon(.,t^n)\|_{L^\infty(\mathbb{R}_x)} \leq \widetilde{C}\varepsilon, \tag{4.34}$$

where the constant $\widetilde{C}$ is uniform and depends only on the underlying wavelet coefficients.

PROOF. The thresholded solution $\texttt{TPE}u_\varepsilon(.,t^n)$ is constant and equal to $\check{v}_{k,j}^{n+1}$ on cells $\Omega_{k,j} \in S_\varepsilon^{n+1}$. Each of these cells is a union of subdivisions $\Omega_{\tilde{k},\tilde{j}} \in \widetilde{S}_\varepsilon^{n+2}$, on which the reconstructed solution $\texttt{RTPE}u_\varepsilon(.,t^n)$ is constant and equal to $v_{\tilde{k},\tilde{j}}^{n+1}$. Therefore,

$$\|\texttt{RTPE}u_\varepsilon(.,t^n) - \texttt{TPE}u_\varepsilon(.,t^n)\|_{L^\infty(\mathbb{R}_x)} = \max_{\substack{(\tilde{k},\tilde{j})\in\partial\widetilde{\Gamma}_\varepsilon^{n+2} \\ \Omega_{\tilde{k},\tilde{j}}\subset\Omega_{k,j} \\ (k,j)\in\partial\Gamma_\varepsilon^{n+1}}} |v_{\tilde{k},\tilde{j}}^{n+1} - \check{v}_{k,j}^{n+1}|. \tag{4.35}$$

By virtue of Lemma 4.2, we obtain

$$|v_{\tilde{k},\tilde{j}}^{n+1} - \check{v}_{k,j}^{n+1}| \leq \widetilde{C}\varepsilon_k \leq \widetilde{C}2^{k-K}\varepsilon \leq \widetilde{C}\varepsilon, \tag{4.36}$$

hence the desired result. □

4.2 Convergence of the sequence of approximate solutions

4.2.1 Statement of the main results

We will now endeavor to apply the five-step methodology described in subsection 2.2 to the sequence of approximate solution (4.8b). This requires us to link the size of the threshold parameter ε with the discretization parameters Δx and Δt. We set

$$\varepsilon = \bar{C}\Delta t. \tag{4.37}$$

The need for this technical constraint on the discretization parameters will appear in the proof of boundedness for the solution, and calls for some justification. First of all, note that a comparable relation between ε and Δx was already found relevant in [6], where the error between the adaptive solution and the reference finite-volume solution on the uniform grid is bounded by an $O(\varepsilon)$-estimate which has a Δt in the numerator. Thanks to the CFL condition, the estimate is therefore in $\varepsilon/\Delta x$. On the other hand, the discretization error of the Godunov scheme is in $\Delta x^{1/2}$. Imposing $\varepsilon = C\Delta x^{1+\theta}$ with $\theta \approx 1/2$ would hence make the two error trends comparable.

In our case, where the ultimate goal a convergence result, we can make the following comment. Suppose the solution u_ε has Hölder smoothness $0 < q \leq N$ in some area containing $\widetilde{\Sigma}_{k,j}$, with N the number of vanishing moments of the dual wavelet. Then standard approximation results in

$$|d_{k,j}| \leq C2^{-qk}\|u\|_{C^q(\widetilde{\Sigma}_{k,j})}. \tag{4.38}$$

Imposing $\varepsilon = \Delta x^{1+\theta}$ therefore amounts to neglecting the details in regions where the solution is $1+\theta$ smooth. This is realistic for solutions of standard hyperbolic PDE away from the discontinuities, and guarantees that our scheme works well with a reasonably sparse adaptive grid.

The first item on our agenda is to derive a uniform L^∞-estimate.

Proposition 4.2. *Consider the Cauchy problem (2.1) with $u_0 \in L^\infty(\mathbb{R}_x)$. For a fixed time $T > 0$, let us consider the CFL restriction*

$$\frac{\Delta t}{2^{-K}\Delta x} \max_{|u| \leq C(T)} \left| f'(u) \right| \leq \frac{1}{2}, \tag{4.39}$$

where

$$C(T) = \|u_0\|_{L^\infty(\mathbb{R}_x)} + \widetilde{C}\bar{C}T, \tag{4.40}$$

in which $\widetilde{C}$ is the constant defined in (4.34) and $\bar{C}$ the constant introduced in (4.37). Then, the sequence of numerical solutions $(u_\varepsilon)_{\varepsilon \geq 0}$ computed by the method (4.9)–(4.15) is uniformly bounded in $L^\infty([0, T[\times\mathbb{R}_x)$ with

$$\|u_\varepsilon\|_{L^\infty(]0,T[\times\mathbb{R}_x)} \leq C(T). \tag{4.41}$$

Note that this estimate is not optimal and in fact rather crude. The linear growth in time is due to the possible fluctuations caused by the refinement operator (4.15), but numerical experiments strongly suggest that, in practice, $C(T)$ is basically constant in time.

From this result, we are in a position to complete STEP 1 and obtain the existence of a Young measure ν that can represent all the weak-$\star$ limits $a(u_\varepsilon)$ of the sequences u_ε chained with any given continuous function $a \in \mathscr{C}^0(\mathbb{R})$. The L^∞-estimate is used again to obtain some bounds on the fluctuations due to the multiresolution operators `T` and `R`. These bounds will then be used to complete the second step of our agenda, namely the convergence of the sequence of approximate solutions.

Theorem 4.1. *Consider the Cauchy problem (2.1) with $u_0 \in L^\infty(\mathbb{R}_x)$. Let $(u_\varepsilon)_{\varepsilon \geq 0}$ be the sequence of approximate solutions computed by the method (4.9)–(4.15). Assume that the discretization parameters ε, Δt, and Δx are such that for any given time $T > 0$, there exists a constant $C_T > 0$, independent of the discretization coefficients, such that*

$$\frac{\Delta x}{\Delta t} + \frac{\varepsilon}{\Delta t} \leq C_T. \tag{4.42}$$

Then, the sequence $(u_\varepsilon)_{\varepsilon \geq 0}$ converges strongly in $L^1_{loc}(]0, T[\times\mathbb{R}_x)$ to the unique entropy weak solution u of (2.1) under the CFL condition (4.39). In other words, for any given time $T > 0$ and any compact $B \subset \mathbb{R}_x$, we have

$$\|u_\varepsilon - u\|_{L^1(]0,T[\times B)} \leq r(\varepsilon), \tag{4.43}$$

where $r(\varepsilon)$ tends to zero in the limit $\varepsilon \to 0$.

4.2.2 Proof of Proposition 4.2

Given $T > 0$ such that $T/\Delta t \in \mathbb{N}^*$, we will consider time indexes such that $0 \leq n \leq T/\Delta t - 1$. Starting from the solution

$$u_\varepsilon(., t^{n+1}) = \mathtt{RTPE} u_\varepsilon(., t^n) \tag{4.44}$$

at time t^{n+1}, we infer that

$$\|u_\varepsilon(., t^{n+1})\|_{L^\infty} \leq \|\mathtt{RTPE} u_\varepsilon(., t^n) - \mathtt{TPE} u_\varepsilon(., t^n)\|_{L^\infty} + \|\mathtt{TPE} u_\varepsilon(., t^n)\|_{L^\infty}. \tag{4.45}$$

Since the maximum principle $\|u_\varepsilon(.,t)\|_{L^\infty} \leq \|u_\varepsilon(.,t^n)\|_{L^\infty}$ is satisfied by the solution of the Cauchy problem for $t \in]t^n, t^{n+1}[$, it is also preserved by the Godunov scheme and the thresholding operation. Therefore,

$$\|\mathtt{TPE}u_\varepsilon(.,t^n)\|_{L^\infty} \leq \|u_\varepsilon(.,t^n)\|_{L^\infty}. \tag{4.46}$$

The remaining term in (4.45) is bounded by the estimate (4.34), namely,

$$\|\mathtt{RTPE}u_\varepsilon(.,t^n) - \mathtt{PE}u_\varepsilon(.,t^n)\|_{L^\infty} \leq \widetilde{C}\varepsilon, \tag{4.47}$$

so that

$$\|u_\varepsilon(.,t^{n+1})\|_{L^\infty} \leq \|u_\varepsilon(.,t^n)\|_{L^\infty} + \widetilde{C}\varepsilon. \tag{4.48}$$

Invoking (4.37), we finally get

$$\|u_\varepsilon(.,t^{n+1})\|_{L^\infty} \leq \|u_{0\varepsilon}\|_{L^\infty} + \widetilde{C}\bar{C}t^{n+1} \leq \|u_0\|_{L^\infty} + \widetilde{C}\bar{C}t^{n+1}. \tag{4.49}$$

The latter inequality holds because the discrete solution $u_{0\varepsilon}$ is obtained from the initial condition u_0 by thresholding and projection, both operations preserving the L^∞-norm. □

4.2.3 Proof of Theorem 4.1

As already mentioned, the proof relies on a sharp evaluation of the discrete entropy inequality satisfied by the approximate solution u_ε. To that purpose, it is worth recalling the following convexity argument which will be heavily used hereafter.

Let $w \in L^\infty(]a,b[)$ be a real-valued function, with $0 < a < b$. Consider its mean value

$$\overline{w} = \frac{1}{b-a}\int_a^b w(y)dy. \tag{4.50}$$

Then, for any given smooth —but not necessarily convex— function $\eta : \mathbb{R} \to \mathbb{R}$, we have

$$\begin{aligned}\frac{1}{b-a}\int_a^b \eta(w(y))dy &= \eta(\overline{w}) \\ &+ \frac{1}{b-a}\int_a^b \Big\{\int_0^1 \eta''(\overline{w} + s(w(y)-\overline{w}))(1-s)ds\Big\}(w(y)-\overline{w})^2 dy.\end{aligned} \tag{4.51}$$

This identity can be readily proved applying Taylor's formula with integral remainder to function η at point $\overline{w}$. It can be seen as a refined version of Jensen's inequality

$$\frac{1}{b-a}\int_a^b \eta(w(y))dy \geq \eta(\overline{w}), \tag{4.52}$$

which is valid only for η convex.

In order to highlight the main ideas, we are going to state three Lemmas and to comment on them, postponing their proofs to the end of the subsection. The first Lemma deals with the entropy inequalities satisfied by the sequence of approximate solutions u_ε.

Lemma 4.3. *For any nonnegative test function $\phi \in \mathscr{C}_c^1(\mathbb{R}_t^+ \times \mathbb{R}_x)$ and for any given entropy/entropy-flux pair (η, q), the entropy weak inequality*

$$\begin{aligned}\int_{\mathbb{R}_x}\eta(u_\varepsilon(x,T))\phi(x,T)dx - \int_{\mathbb{R}_x}\eta(u_\varepsilon^0(x))\phi(x,0)dx - \int_0^T\int_{\mathbb{R}_x}\big\{\eta(u_\varepsilon)\partial_t\phi + q(u_\varepsilon)\partial_x\phi\big\}(x,t)dxdt \\ \leq \sum_{n=0}^N \int_{\mathbb{R}_x}\big[\eta(\mathtt{RTPE}u_\varepsilon) - \eta(\mathtt{E}u_\varepsilon)\big](x,t^n)\phi(x,t^{n+1})dx\end{aligned} \tag{4.53}$$

holds under the CFL restriction (4.39).

The left-hand side of (4.53) can be easily handled in the limit $\varepsilon \to 0$ thanks to the Young measure $\nu_{x,t}$ associated with the uniformly bounded sequence of approximate solutions $(u_\varepsilon)_{\varepsilon>0}$. The right-hand side can interpreted as an error term, which has to be shown to decay to 0 with ε. To achieve this purpose, we split this error term into two contributions by inserting $\eta(\mathtt{TPE}u_\varepsilon)$ into the integrand, that is,

$$\begin{aligned}\sum_{n=0}^{N}\int_{\mathbb{R}_x}\big[\eta(\mathtt{RTPE}u_\varepsilon)-\eta(\mathtt{E}u_\varepsilon)\big](x,t^n)\phi(x,t^{n+1})dx&\\ =\sum_{n=0}^{N}\int_{\mathbb{R}_x}\big[\eta(\mathtt{RTPE}u_\varepsilon)-\eta(\mathtt{TPE}u_\varepsilon)\big](x,t^n)\phi(x,t^{n+1})dx&\\ +\sum_{n=0}^{N}\int_{\mathbb{R}_x}\big[\eta(\mathtt{TPE}u_\varepsilon)-\eta(\mathtt{E}u_\varepsilon)\big](x,t^n)\phi(x,t^{n+1})dx.&\end{aligned}\tag{4.54}$$

The first contribution in (4.54) is due to the refinement operator R. Its control, as the threshold parameter ε goes to zero, is the matter of the next Lemma.

Lemma 4.4. *For any test function $\phi \in \mathscr{C}_c^1(\mathbb{R}_t^+ \times \mathbb{R}_x)$ and for any smooth function η, the estimate*

$$\sum_{n=0}^{N}\int_{\mathbb{R}_x}\big[\eta(\mathtt{RTPE}u_\varepsilon)-\eta(\mathtt{TPE}u_\varepsilon)\big](x,t^n)\phi(x,t^{n+1})dx \le C\varepsilon||\phi||_{L^\infty(\mathbb{R}_t^+,W^{1,\infty}(\mathbb{R}_x))}\tag{4.55}$$

holds under assumption (4.42) of Theorem 4.1, where $C>0$ is some uniform constant.

The second contribution in the entropy production term (4.54) stems from the averaging procedures performed at each time step, namely the projection step P on the grid $S(\tilde{\Gamma}_\varepsilon^{n+1})$ followed by the multiresolution thresholding T on the coarser grid $S(\Gamma_\varepsilon^{n+1})$. This term is controlled thanks to

Lemma 4.5. *For any nonnegative test function $\phi \in \mathscr{C}_c^1(\mathbb{R}_t^+ \times \mathbb{R}_x)$ and for any smooth convex function η, the estimate*

$$\sum_{n=0}^{N}\int_{\mathbb{R}_x}\big[\eta(\mathtt{TPE}u_\varepsilon)-\eta(\mathtt{E}u_\varepsilon)\big](x,t^n)\phi(x,t^{n+1})dx \le C\varepsilon^{1/2}\|\phi\|_{L^\infty(\mathbb{R}_t^+,W^{1,\infty}(\mathbb{R}_x))}\tag{4.56}$$

holds under the CFL condition (4.39), where $C>0$ is some uniform constant.

As an immediate consequence of estimates (4.55)–(4.56), the entropy weak inequality (4.53) becomes

$$\int_0^T\int_{\mathbb{R}_x}\big\{\eta(u_\varepsilon)\partial_t\phi+q(u_\varepsilon)\partial_x\phi\big\}(x,t)dxdt+C\varepsilon^{1/2}\|\phi\|_{L^\infty(\mathbb{R}_t^+,W^{1,\infty}(\mathbb{R}_x))}\ge 0,\tag{4.57}$$

for any given non-negative test function $\phi \in \mathscr{C}_c^1(]0,T[\times\mathbb{R}_x)$ (which implies $\phi(x,0)=\phi(x,T)=0$). This immediately gives rise to

$$\int_0^T\int_{\mathbb{R}_x}\big\{\langle\nu_{x,t},\eta\rangle\partial_t\phi(x,t)+\langle\nu_{x,t},q\rangle\partial_x\phi(x,t)\big\}dxdt\ge 0\tag{4.58}$$

in the limit $\varepsilon \to 0$ for any given entropy/entropy-flux pair (η, q). In other words, ν is nothing but an entropy measure-valued solution. Standard arguments based on the weak BV-estimate in Theorem A.2 proves that ν assumes its initial data $\delta_{u0(x)}$ in the strong sense (the reader is referred to [10]). By the DiPerna theorem, the measure $\nu_{x,t}$ thus coincides with $\delta_{u(x,t)}$ for some bounded function $u(x,t)$, which in turn can only be the Kruzkov solution of the Cauchy problem (2.1). This proves the strong convergence of the discrete method.

We now proceed with the proofs of the three above Lemmas.

Proof of Lemma 4.3. During the evolution step $\mathtt{E}$, the exact entropy weak solution of the Cauchy problem (2.1a) with initial data $u_\varepsilon(x,t^n)$ is used on the time interval $[t^n, t^{n+1}[$ to arrive at $\mathtt{E}u_\varepsilon(x,t^n)$. For any given non-negative test function $\phi \in \mathscr{C}^1_c(\mathbb{R}^+_t \times \mathbb{R}_x)$, this just reads

$$-\int_{t^n}^{t^{n+1}}\int_{\mathbb{R}_x} \big\{\eta(u_\varepsilon)\partial_t\phi + q(u_\varepsilon)\partial_x\phi\big\}(x,t)dxdt \qquad (4.59)$$
$$+\int_{\mathbb{R}_x} \eta(\mathtt{E}u_\varepsilon(x,t^n))\phi(x,t^{n+1})dx - \int_{\mathbb{R}_x}\big\{\eta(u_\varepsilon)\phi\big\}(x,t^n)dx \le 0.$$

Let us add these inequalities together for $n \in \{0,...,N\}$, with $N = T/\Delta t - 1$, swap the order of summation and insert

$$\eta(u_\varepsilon)(x,t^{n+1})\phi(x,t^n) = \{\eta(\mathtt{RTPE}u_\varepsilon)\phi\}(x,t^n) \qquad (4.60)$$

into both sides. This yields

$$\int_{\mathbb{R}_x}\sum_{n=0}^{N}\big[\big\{\eta(u_\varepsilon)\phi\big\}(x,t^{n+1}) - \big\{\eta(u_\varepsilon)\phi\big\}(x,t^n)\big]dx - \int_0^T\int_{\mathbb{R}_x}\big\{\eta(u_\varepsilon)\partial_t\phi + q(u_\varepsilon)\partial_x\phi\big\}(x,t)dxdt$$
$$\le \int_{\mathbb{R}_x}\sum_{n=0}^{N}\big[\eta(\mathtt{RTPE}u_\varepsilon) - \eta(\mathtt{E}u_\varepsilon)\big](x,t^n)\phi(x,t^{n+1})dx. \qquad (4.61)$$

After simplifying the telescoping sum in the left-hand side, we obtain (4.53). □

Proof of Lemma 4.4. Let us introduce the piecewise-constant version of the test function ϕ, that is,

$$\phi_\varepsilon(x,t^n) \equiv \phi^n_{k,j} = \frac{1}{\Delta x_k}\int_{\Omega_{k,j}}\phi(x,t^n)dx, \qquad \text{for } \ x \in \Omega_{k,j}, \quad (k,j) \in \partial\Gamma^{n+1}_\varepsilon. \qquad (4.62)$$

Then, the identity

$$\int_{\mathbb{R}_x}\big[\eta(\mathtt{RTPE}u_\varepsilon) - \eta(\mathtt{TPE}u_\varepsilon)\big](x,t^n)\phi(x,t^{n+1})dx$$
$$= \int_{\mathbb{R}_x}\big[\eta(\mathtt{RTPE}u_\varepsilon) - \eta(\mathtt{TPE}u_\varepsilon)\big](x,t^n)\big[\phi - \phi_\varepsilon\big](x,t^{n+1})dx$$
$$+ \sum_{(k,j)\in\partial\Gamma^{n+1}_\varepsilon}\phi^{n+1}_{k,j}\int_{\Omega_{k,j}}\big[\eta(\mathtt{RTPE}u_\varepsilon) - \eta(\mathtt{TPE}u_\varepsilon)\big](x,t^n)dx \qquad (4.63)$$

occurs by inserting ϕ_ε into the left-hand side. The last term in the right-hand side can be bounded by

$$\begin{aligned}\int_{\Omega_{k,j}} \big[\eta(\mathtt{RTPE}u_\varepsilon) - \eta(\mathtt{TPE}u_\varepsilon)\big](x,t^n)dx &= \int_{\Omega_{k,j}} \eta(\mathtt{RTPE}u_\varepsilon(x,t^n))dx - \eta(\check{v}_{k,j}^{n+1})\Delta x_k \\ &\leq \|\eta''(u_\varepsilon)\|_{L^\infty([0,T]\times\mathbb{R}_x)} \big\|\big\{\mathtt{RTPE}u_\varepsilon - \mathtt{TPE}u_\varepsilon\big\}(.,t^n)\big\|^2_{L^\infty(\mathbb{R}_x)}\Delta x_k \\ &\leq \tilde{C}^2\|\eta''(u_\varepsilon)\|_{L^\infty([0,T]\times\mathbb{R}_x)}\varepsilon^2\Delta x_k \end{aligned} \tag{4.64}$$

using successively the refined version (4.51) of Jensen's inequality, the sup-norm estimate (4.41) of Proposition 4.2 and the estimate (4.34) of Proposition 4.1. We thus find

$$\begin{aligned}\sum_{(k,j)\in\partial\Gamma_\varepsilon^{n+1}} \phi_{k,j}^{n+1} \int_{\Omega_{k,j}} \big[\eta(\mathtt{RTPE}u_\varepsilon) - \eta(\mathtt{TPE}u_\varepsilon)\big](x,t^n)dx& \\ \leq C\varepsilon^2\|\phi(.,t^{n+1})\|_{L^\infty(\mathbb{R}_x)}\,|\mathrm{supp}\,\phi(.,t^{n+1})|.& \end{aligned} \tag{4.65}$$

By performing similar steps, we can deal with the first term in (4.63) according to

$$\begin{aligned}\int_{\mathbb{R}_x} \big[\eta(\mathtt{RTPE}u_\varepsilon) - \eta(\mathtt{TPE}u_\varepsilon)\big](x,t^n)\big[\phi-\phi_\varepsilon\big](x,t^{n+1})dx& \\ \leq \tilde{C}\varepsilon\Delta x\|\eta'(u_\varepsilon)\|_{L^\infty}\|\partial_x\phi(.,t^{n+1})\|_{L^\infty(\mathbb{R}_x)}\,|\mathrm{supp}\,\phi(.,t^{n+1})|& \\ \leq C\varepsilon\Delta x\|\partial_x\phi(.,t^{n+1})\|_{L^\infty(\mathbb{R}_x)}\,|\mathrm{supp}\,\phi(.,t^{n+1})|.& \end{aligned} \tag{4.66}$$

Plugging the bounds (4.65) and (4.66) into (4.63) provides the estimate

$$\begin{aligned}\int_{\mathbb{R}_x} \big[\eta(\mathtt{RTPE}u_\varepsilon) - \eta(\mathtt{TPE}u_\varepsilon)\big](x,t^n)\phi(x,t^{n+1})dx& \\ \leq C(\varepsilon\Delta x+\varepsilon^2)\|\phi(.,t^{n+1})\|_{W^{1,\infty}(\mathbb{R}_x)}\,|\mathrm{supp}\,\phi(.,t^{n+1})|.& \end{aligned} \tag{4.67}$$

Again, we add these inequalities for n ranging from 0 to N (while keeping in mind that $N+1 = T/\Delta t$), swap the order of summation and invoke assumption (4.42) to get

$$\begin{aligned}\sum_{n=0}^{N}\int_{\mathbb{R}_x} \big[\eta(\mathtt{RTPE}u_\varepsilon) - \eta(\mathtt{TPE}u_\varepsilon)\big](x,t^n)\phi(x,t^{n+1})dx& \\ \leq C\varepsilon T\Big(\frac{\Delta x}{\Delta t}+\frac{\varepsilon}{\Delta t}\Big)\|\phi\|_{L^\infty(\mathbb{R}_t,W^{1,\infty}(\mathbb{R}_x))}& \\ \leq C\varepsilon\|\phi\|_{L^\infty(\mathbb{R}_t,W^{1,\infty}(\mathbb{R}_x))}.& \end{aligned} \tag{4.68}$$

This completes the proof. □

The proof of Lemma 4.5 is somewhat more intricate. It relies on a preliminary weak BV-like estimate.

Lemma 4.6. *Let $T>0$ be any given fixed time and let B be any given compact interval of $\mathbb{R}_x$. Then, under the CFL condition (4.39), there exists a positive constant C independent of ε such that*

$$\sum_{n=0}^{N}\int_B |\mathtt{E}u_\varepsilon - \mathtt{TPE}u_\varepsilon|^2(x,t^n)dx \leq C. \tag{4.69}$$

Proof of Lemma 4.5. Let us again consider the nonnegative discrete test function $\phi_\varepsilon(x,t)$ introduced in (4.62). Then, the identity

$$\begin{aligned}\int_{\mathbb{R}_x} \big[\eta(\mathtt{TPE}u_\varepsilon) - \eta(\mathtt{E}u_\varepsilon)\big](x,t^n)\phi(x,t^{n+1})dx \\ = \int_{\mathbb{R}_x} \big[\eta(\mathtt{TPE}u_\varepsilon) - \eta(\mathtt{E}u_\varepsilon)\big](x,t^n)\big[\phi-\phi_\varepsilon\big](x,t^{n+1})dx \\ + \sum_{(k,j)\in\partial\Gamma_\varepsilon^{n+1}} \phi_{k,j}^{n+1}\int_{\Omega_{k,j}} \big[\eta(\mathtt{TPE}u_\varepsilon) - \eta(\mathtt{E}u_\varepsilon)\big](x,t^n)dx \end{aligned} \tag{4.70}$$

occurs by inserting ϕ_ε into the left-hand side. By construction, $\mathtt{TPE}u_\varepsilon(x,t^n)$ remains constant on each cell $\Omega_{k,j}$, $(k,j)\in\partial\Gamma_\varepsilon^{n+1}$, with the property

$$\frac{1}{\Delta x_k}\int_{\Omega_{k,j}} \big[\mathtt{E}u_\varepsilon - \mathtt{TPE}u_\varepsilon\big](x,t^n)dx = \frac{1}{\Delta x_k}\int_{\Omega_{k,j}} \mathtt{E}u_\varepsilon(x,t^n)dx - \check{v}_{k,j}^{n+1} = 0. \tag{4.71}$$

Consequently, the last term in the right-hand side of (4.70) vanishes. Furthermore, the refined version (4.51) of Jensen's inequality ensures

$$\frac{1}{\Delta x_k}\int_{\Omega_{k,j}} \big[\eta(\mathtt{TPE}u_\varepsilon) - \eta(\mathtt{E}u_\varepsilon)\big](x,t^n)dx \le 0. \tag{4.72}$$

It follows from (4.70) the estimate

$$\int_{\mathbb{R}_x} \big[\eta(\mathtt{TPE}u_\varepsilon) - \eta(\mathtt{E}u_\varepsilon)\big](x,t^n)\phi(x,t^{n+1})dx \tag{4.73}$$

$$\le \int_{\mathbb{R}_x} |\eta(\mathtt{TPE}u_\varepsilon) - \eta(\mathtt{E}u_\varepsilon)|(x,t^n)\cdot|\phi-\phi_\varepsilon|(x,t^{n+1})dx, \tag{4.74}$$

valid for all nonnegative test function ϕ. Let us use the crude estimate

$$|\phi-\phi_\varepsilon|(x,t^{n+1}) \le \frac{1}{\Delta x_k}\int_{\Omega_{k,j}} |\phi(x,t^{n+1}) - \phi(y,t^{n+1})|dy \tag{4.75}$$

$$\le \Delta x ||\partial_x\phi(.,t^{n+1})||_{L^\infty(\mathbb{R}_x)}\chi\circ\phi_\varepsilon(x,t^{n+1}), \tag{4.76}$$

valid for all $x\in\Omega_{(k,j)}$, $(k,j)\in\partial\Gamma_\varepsilon^{n+1}$, where we have introduced the characteristic function

$$\chi\circ\phi(x,t^{n+1}) = \begin{cases} 1 & \text{if } x\in \text{ supp}\,\phi(.,t^{n+1}), \\ 0 & \text{otherwise.}\end{cases} \tag{4.77}$$

From (4.73), we infer the following bound

$$\int_{\mathbb{R}_x} \big[\eta(\mathtt{TPE}u_\varepsilon) - \eta(\mathtt{E}u_\varepsilon)(x,t^n)\big]\phi(x,t^{n+1})dx \tag{4.78}$$

$$\le C_T\|\eta'(u_\varepsilon)\|_{L^\infty}\|\partial_x\phi(.,t^{n+1})\|_{L^\infty}\Delta t\sum_{n=0}^{N}\int_{\mathbb{R}_x} |\mathtt{E}u_\varepsilon - \mathtt{TPE}u_\varepsilon|(x,t^n)\chi\circ\phi_\varepsilon(x,t^{n+1})dx,$$

where, in view of assumption (4.42), we have replaced Δx by $C_T\Delta t$. It now suffices to apply the Cauchy-Schwarz inequality in both time and space to get

$$\begin{aligned}\Delta t\sum_{n=0}^{N}\int_{\mathbb{R}_x}|\mathtt{E}u_\varepsilon-\mathtt{TPE}u_\varepsilon|(x,t^n)\chi\circ\phi_\varepsilon(x,t^{n+1})dx&\\ \le|\mathrm{supp}\,\phi|^{1/2}\Big(\Delta t\sum_{n=0}^{N+1}\int_{\mathbb{R}_x}|\mathtt{E}u_\varepsilon-\mathtt{TPE}u_\varepsilon|^2(x,t^n)\chi\circ\phi_\varepsilon(x,t^{n+1})dx\Big)^{1/2}&\\ \le C\Delta t^{1/2},&\end{aligned}\tag{4.79}$$

where we have used the estimate (4.69) of Lemma 4.6. □

Proof of Lemma 4.6. Let $\psi:y\in\mathbb{R}^+\to\psi(y)\in[0,1]$ be a smooth function satisfying

$$\psi(y)=1\quad\text{for }\ 0\le y\le 1,\qquad\psi(y)=0\quad\text{for }\ y\ge 2.\tag{4.80}$$

Given any fixed compact B on which we want to show (4.69), we define a space index

$$r\in\mathbb{N}\quad\text{such that}\quad B\subset\mathscr{B}(0,R),\quad R=(r+1)\Delta x.\tag{4.81}$$

We then consider the nonnegative test function

$$\phi(x,t)=\psi_T(t)\psi_R(x)=\psi\Big(\frac{t}{T}\Big)\psi\Big(\frac{|x|}{R}\Big)\tag{4.82}$$

in $\mathscr{C}^1_c(\mathbb{R}^+_t\times\mathbb{R}_x)$. Observe that $\phi(x,t)$ boils down to $\psi_R(x)$ for all time $t\in[0,T]$. Applying the inequality (4.53) of Lemma 4.3 with the splitting (4.54) and the convex entropy function $\eta(u)=u^2$ yields

$$\begin{aligned}\int_{\mathbb{R}_x}|u_\varepsilon(x,T)|^2\psi_R(x)dx+\sum_{n=0}^{N}\int_{\mathbb{R}_x}\big[|\mathtt{E}u_\varepsilon|^2-|\mathtt{TPE}u_\varepsilon|^2\big](x,t^n)\psi_R(x)dx&\\ \le\int_{\mathbb{R}_x}|u_\varepsilon(x,0)|^2\psi_R(x)dx+\int_0^T\int_{\mathbb{R}_x}q(u_\varepsilon(x,t))\partial_x\psi_R(x)dxdt&\\ +\sum_{n=0}^{N}\int_{\mathbb{R}_x}\big[|\mathtt{RTPE}u_\varepsilon|^2-|\mathtt{TPE}u_\varepsilon|^2\big](x,t^n)\psi_R(x)dx.&\end{aligned}\tag{4.83}$$

Combining this and the estimate (4.55) of Lemma 4.4, we have

$$\begin{aligned}\sum_{n=0}^{N}\int_{\mathbb{R}_x}\big[|\mathtt{E}u_\varepsilon|^2-|\mathtt{TPE}u_\varepsilon|^2\big](x,t^n)\psi_R(x)dx&\\ \le R\|u_0\|^2_{L^\infty}\|\psi\|_{L^1(\mathbb{R}^+)}+T\|q(u_\varepsilon)\|_{L^\infty}\|\partial_x\psi\|_{L^1(\mathbb{R}^+)}+CTR\varepsilon\|\psi\|_{W^{1,\infty}(\mathbb{R}^+)}.&\end{aligned}\tag{4.84}$$

Introducing the piecewise-constant version $\psi_{R,\varepsilon}$ of ψ_R, defined as in (4.62), we deduce from (4.84) that

$$\begin{aligned}\sum_{n=0}^{N}\int_{\mathbb{R}_x}\big[|\mathtt{E}u_\varepsilon|^2-|\mathtt{TPE}u_\varepsilon|^2\big](x,t^n)\psi_{R,\varepsilon}(x)dx&\\ \le C+C\sum_{n=0}^{N}\sum_{(k,j)\in\partial\Gamma_\varepsilon^{n+1}}\int_{\Omega_{k,j}}\big[|\mathtt{E}u_\varepsilon|^2-|\mathtt{TPE}u_\varepsilon|^2\big](x,t^n)\cdot\big[\psi_{R,\varepsilon}-\psi_R\big](x)dx,&\end{aligned}\tag{4.85}$$

so that going along the same lines as those used to obtain (4.78), we get

$$\sum_{n=0}^{N}\int_{\mathbb{R}_x}\big[|\mathtt{E}u_\varepsilon|^2-|\mathtt{TPE}u_\varepsilon|^2\big](x,t^n)\psi_{R,\varepsilon}(x)dx\le C+C\|u_\varepsilon\|_{L^\infty}^2\Delta t\sum_{n=0}^{N}\int_{\mathbb{R}_x}\chi\circ\psi_R(x)dx,$$
$$\le C. \tag{4.86}$$

Each summand in the left-hand side of (4.86) can be decomposed as

$$\int_{\mathbb{R}_x}\big[|\mathtt{E}u_\varepsilon|^2-|\mathtt{TPE}u_\varepsilon|^2\big](x,t^n)\psi_{R,\varepsilon}(x)dx=\sum_{(k,j)\in\partial\Gamma_\varepsilon^{n+1}}(\psi_{R,\varepsilon})_{k,j}^n\int_{\Omega_{k,j}}\big[|\mathtt{E}u_\varepsilon(x,t^n)|^2-|\check{v}_{k,j}^{n+1}|^2\big]dx, \tag{4.87}$$

which demonstrates that it is the sum of nonnegative terms, for

$$\int_{\Omega_{k,j}}\big[|\mathtt{E}u_\varepsilon(x,t^n)|^2-|\check{v}_{k,j}^{n+1}|^2\big]dx\ge 0 \tag{4.88}$$

according to Jensen's inequality on the finite interval $\Omega_{k,j}$. Because of nonnegativity, any partial sum extracted from the right-hand side of (4.87) will be lesser than its left-hand side. Since

$$\int_{-R}^{R}\big[|\mathtt{E}u_\varepsilon|^2-|\mathtt{TPE}u_\varepsilon|^2\big](x,t^n)dx=\sum_{(k,j)\in\partial\Gamma_\varepsilon^{n+1}}\int_{\Omega_{k,j}\cap[-R,R]}\big[|\mathtt{E}u_\varepsilon(x,t^n)|^2-|\check{v}_{k,j}^{n+1}|^2\big]dx$$

and since the intersection set $\Omega_{k,j}\cap[-R,R]$ is either $\Omega_{k,j}$ or $\emptyset$ by the choice (4.81) for R, the above quantity is indeed a partial sum extracted from (4.87), corresponding to the test function $\psi_{R,\varepsilon}$ selected in (4.80). Hence, using (4.86), we have the uniform estimate

$$\sum_{n=0}^{N}\int_{-R}^{R}\big[|\mathtt{E}u_\varepsilon|^2-|\mathtt{TPE}u_\varepsilon|^2\big](x,t^n)dx\le C. \tag{4.89}$$

Once again, we resort to the extended version (4.51) of Jensen's inequality to find

$$\begin{aligned}\int_{-R}^{R}\big[|\mathtt{E}u_\varepsilon|^2-|\mathtt{TPE}u_\varepsilon|^2\big](x,t^n)dx&=2\sum_{(k,j)\in\partial\Gamma_\varepsilon^{n+1}}\int_{\Omega_{k,j}\cap[-R,R]}|\mathtt{E}u_\varepsilon(x,t^n)-\check{v}_{k,j}^{n+1}|^2dx\\&=2\int_{-R}^{R}|\mathtt{E}u_\varepsilon-\mathtt{TPE}u_\varepsilon|^2(x,t^n)dx.\end{aligned} \tag{4.90}$$

Substituting this identity into (4.89) provides the required weak BV-estimate (4.69), since we have chosen R large enough with respect to the compact interval B. □

5 Local Time Stepping enhancement

5.1 Description of the numerical scheme

We now describe the Local Time Stepping enhancement. The idea is to use a time-step locally adapted to the size of the cell —satisfying in particular the CFL stability condition. In our case where the multiresolution scheme is based on a hierarchy of nested dyadic grids, the major ingredient of the method is the design of a macroscopic time-step suitable for the

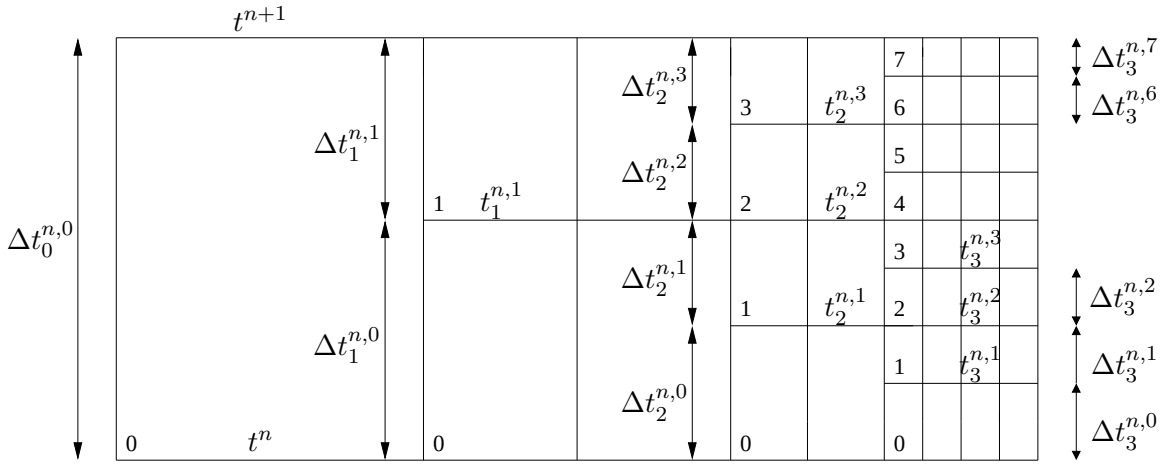

Figure 4: A four-level adaptive grid, with the level dependent intermediate time step numbering

coarsest level cells, along with a cascade of intermediate time-steps at which the solution defined on finer levels is updated in turn. Figure 4 illustrates this idea in the case of a four-level hierarchy.

For an arbitrary number K of levels, the macro time-step is subdivided into 2^K intermediate steps, which we shall be referring to with a double time superscript on the k-level, i.e.,

$$t_k^{n,i+1} = t_k^{n,i} + \Delta t_k^{n,i}, \quad \text{for } \; i = 0, \ldots, 2^k - 1. \tag{5.1}$$

The intermediate time-steps are all synchronized at the macro time-step, i.e.,

$$t_k^{n,0} = t^n, \qquad t_k^{n,2^k} = t^{n+1}, \tag{5.2}$$

and also synchronized every other time-step between consecutive levels because of

$$\Delta t_{k-1}^{n,i} = \Delta t_k^{n,2i} + \Delta t_k^{n,2i+1}, \tag{5.3}$$

which leads to

$$t_{k-1}^{n,i} = t_k^{n,2i}. \tag{5.4}$$

The cells on the finest level K are updated from time $t_K^{n,i}$ to time $t_K^{n,i+1}$ with a time-step $\Delta t_K^{n,i}$. In practice, we will use this finest time grid as the reference grid and we will denote it by $t^{n,i+1}$ (with the corresponding time step $\Delta t^{n,i}$) to alleviate the notations. Applying the CFL stability condition (2.8) can impose the elementary time-step to decrease during a macro time-step. Moreover, we will see that it is necessary to reduce the coefficient from 1/2 to 1/3 to ensure that discontinuities coming from consecutive cell interfaces do not interfere. Therefore, we impose in the sequel

$$\frac{\Delta t^{n,i}}{2^{-K}\Delta x_0} \max_{|u| \le C(T)} |f'(u)| \le \frac{1}{3} \tag{5.5}$$

with $C(T)$ given by (4.40). At time $t^{n,i}$, the smallest synchronization level is determined by

$$k_i := \min\{k\,; \;\; 0 \le k \le K, \;\; i \equiv 0 \; [2^{K-k}]\}. \tag{5.6}$$

As illustrated on the four-level hierarchy example depicted in Figure 4, all cells belonging to levels finer than or equal to k_i are updated during the intermediate step i. Two cases must be considered depending on whether those cells belong or not to the range of dependence Σ_ℓ of finer cells. The range of dependence Σ_ℓ of a cell ℓ on level k is determined by the stencil of the $2r$-point finite-volume numerical flux and the multiscale local prediction (3.5) as a set of cells on level $k-1$

$$\Sigma_\ell := \big\{ \lfloor (\ell - r)/2 \rfloor - 1, \ldots, \lfloor (\ell + r)/2 \rfloor + 1 \big\}. \tag{5.7}$$

The partial updating at level k acts on active cells at this level, whose indices are in

$$\widetilde{\mathcal{I}}_k := \big\{ (k,j); (k,j) \in \partial\widetilde{\Gamma}_\varepsilon^{n+1} \big\}. \tag{5.8}$$

This set of indices is split into two disjoint sets $\widetilde{\mathcal{I}}_k = \mathcal{C}_k \cup \overline{\mathcal{C}}_k$. The index set $\mathcal{C}_k$ contains those cells at level k that can be evolved in time by one time-step with step size $\Delta t_k^{n,i} = 2^{K-k}\Delta t^{n,i}$, without having to access data on finer levels in order to compute the fluxes. The complementary set $\overline{\mathcal{C}}_k$ contains those cells at level k that are close to cells on level $k+1$. Something special must be done there, in order to provide the synchronized data necessary to compute all the fluxes on level $k+1$.

To sum it up, at each intermediate time step the index sets are designed with Algorithm 5.1, in accordance with the evolution of the grid $\widetilde{\mathcal{S}}_\varepsilon^{n,i+1}$. The partial update procedure of the adaptive grid at intermediate time steps will be detailed later on.

Algorithm 6 Definition of index sets

On the finest level K all cells in the adaptive grid are evolved
$\mathcal{C}_K := \big\{ (K,j); (K,j) \in \partial\widetilde{\Gamma}_\varepsilon^{n,i+1} \big\} = \widetilde{\mathcal{I}}_K$.
for $k = K-1 \searrow 0$ **do**
  $\mathcal{C}_k := \big\{ (k,j), (k,j) \in \partial\widetilde{\Gamma}_\varepsilon^{n,i+1}; \nexists \ell, (k+1,\ell) \in \partial\widetilde{\Gamma}_\varepsilon^{n,i+1} : j \in \Sigma_\ell \big\}$,
  $\overline{\mathcal{C}}_k := \widetilde{\mathcal{I}}_k \backslash \mathcal{C}_k$,
end for

From the standpoint of analysis, the cornerstone is the synchronization of the solution on cells at the boundary between different levels of discretization. We summarize two possibilities that have been proposed in the literature [26, 29] on a two-level example sketched on Figures 6 and 5. To alleviate the notations we deliberately omit the subscript ε for the discrete solution.

In [29], Osher and Sanders first update the solution of the small cell $\Omega_{1,2j+2}$ of size $\Delta x_1 = \Delta x_0/2$ over a time step $\Delta t_1^{n,0}$ using fluxes computed with solution at time n on cells $\Omega_{0,j}$, $\Omega_{1,2j+2}$, $\Omega_{1,2j+3}$. The solution in the transition zone, here the first cell neighboring the fine level 1, is left unchanged (see Figure 5). It is used again to update the flux entering in the evolution of the solution on the cell $\Omega_{1,2j+2}$ from time $t_1^{n,1}$ to time t^{n+1}. In [26], Müller and Stiriba introduce a transition zone neighboring smaller cells region where the solution is updated using the time-step adapted to the small cells. In the example on Figure 6 the solution on the coarse cell $\Omega_{0,j}$ in the intermediate zone is updated at time step $t_1^{n,1}$, in order to keep the solution synchronized. To update the solution from time $t_1^{n,1}$ to time t^{n+1} a new flux is computed for interface $(0, j+1/2)$, using the solution $v_{0,j}^{n,1}$ and $v_{1,2j+2}^{n,1}$. On the other hand, the flux at interface $(0, j-1/2)$ is valid throughout the full time step $\Delta t^{n,0} + \Delta t^{n,1}$ and is not updated.

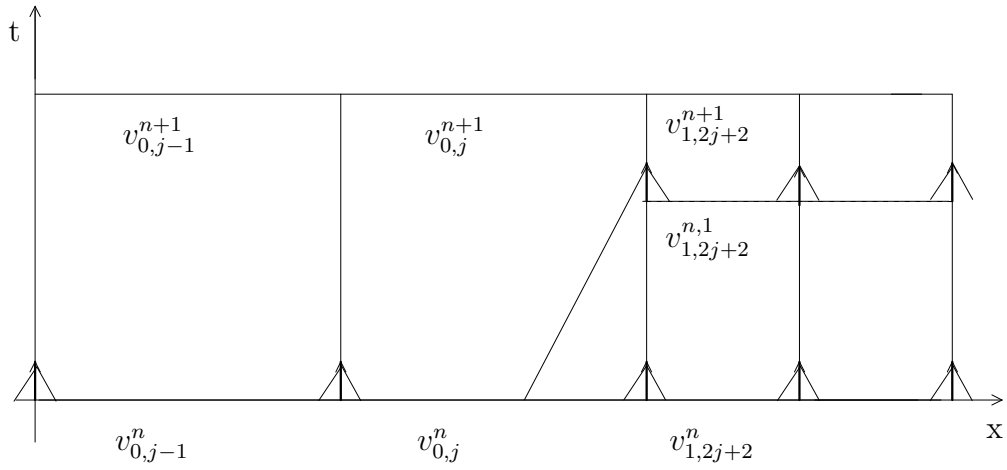

Figure 5: Treatment of the transition zone by Oshers-Sanders [29]

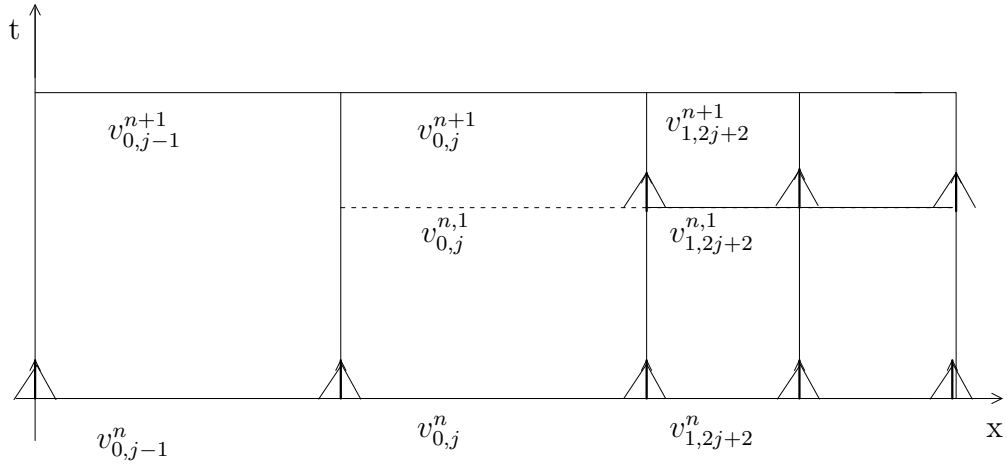

Figure 6: Treatment of the transition zone by Müller and Stiriba [26]

Both schemes of Osher-Sanders and Müller-Stiriba are conservative. The Osher-Sanders scheme has been proved to be entropy-satisfying in the scalar case using monotonicity arguments but nothing is known in the case of systems. We now propose a new approach which does satisfy discrete entropy inequalities in the general case. This approach comes within the spirit of the Godunov analysis [16], and therefore applies to the scalar as well as system settings. We will describe it in detail in the case of the example sketched in Figure 7. Unlike the two other approaches, at time t^n the transition zone is cut in half and the solution in each half-cell is set equal to the solution in the mother cell $\Omega_{0,j}$ (see Figure 8a). The Cauchy problem is then solved for the first intermediate time step (see Figure 8b). Its solution is averaged only on the cell that belongs to the stencil of finer cells, and of course on the fine cells themselves (see Figure 8c). Therefore the updating goes as

$$v^{n,1}_{1,2j+1} = v^n_{0,j} - \frac{2\Delta t^{n,0}_1}{\Delta x_0}\big(\hat{F}(v^n_{0,j}, v^n_{1,2j+2}) - \hat{F}(v^n_{0,j}, v^n_{0,j})\big). \tag{5.9}$$

At this point, the fluxes needed to advance the solution on the fine cell $\Omega_{1,2j+2}$ can be updated using the synchronized solution at the intermediate time-step. The Cauchy problem

for the second intermediate time-step is then solved. It starts from the averaged solution on the cell $\Omega_{1,2j+1}$ and from the non-averaged one on the cell $\Omega_{1,2j}$. Due to the special CFL condition (5.5), chosen lower to 1/3 the data coming from interfaces $(0, j-1/2)$ and $(1, 2j+1/2)$ cannot interact (see Figures 7 and 8d). The solution of the Cauchy problem is then time averaged like in the Godunov scheme to obtain the discrete solution at time $t^{n,2} = t^{n+1}$ (see Figure 8e). At the discrete level, combining the evolution and projection operator leads to the scheme

$$v_{1,2j+2}^{n+1} = v_{1,2j+2}^{n,1} - \frac{2\Delta t_1^{n,1}}{\Delta x_0}\big(\hat{F}(v_{1,2j+2}^{n,1}, v_{1,2j+3}^{n,1}) - \hat{F}(v_{1,2j+1}^{n,1}, v_{1,2j+2}^{n,1})\big). \tag{5.10}$$

on the fine cell $\Omega_{1,2j+2}$. On the coarse cell $\Omega_{0,j}$ in the transition zone, the solution is eventually updated directly from t^n to t^{n+1} as

$$\begin{aligned} v_{0,j}^{n+1} = v_{0,j}^{n} - \frac{1}{\Delta x_0}\big(&\Delta t_1^{n,0}\hat{F}(v_{0,j}^{n}, v_{1,2j+2}^{n}) + \Delta t_1^{n,1}\hat{F}(v_{1,2j+1}^{n,1}, v_{1,2j+2}^{n,1}) \\ &- \Delta t_0^{n,0}\hat{F}(v_{0,j-1}^{n}, v_{0,j}^{n})\big). \end{aligned} \tag{5.11}$$

The solution on the coarse cells outside the transition zone is directly updated from time-step t^n to time-step t^{n+1} as

$$v_{0,j-1}^{n+1} = v_{0,j-1}^{n} - \frac{\Delta t_0^{n,0}}{\Delta x_0}\big(\hat{F}(v_{0,j-1}^{n}, v_{0,j}^{n}) - \hat{F}(v_{0,j-2}^{n}, v_{0,j-1}^{n})\big). \tag{5.12}$$

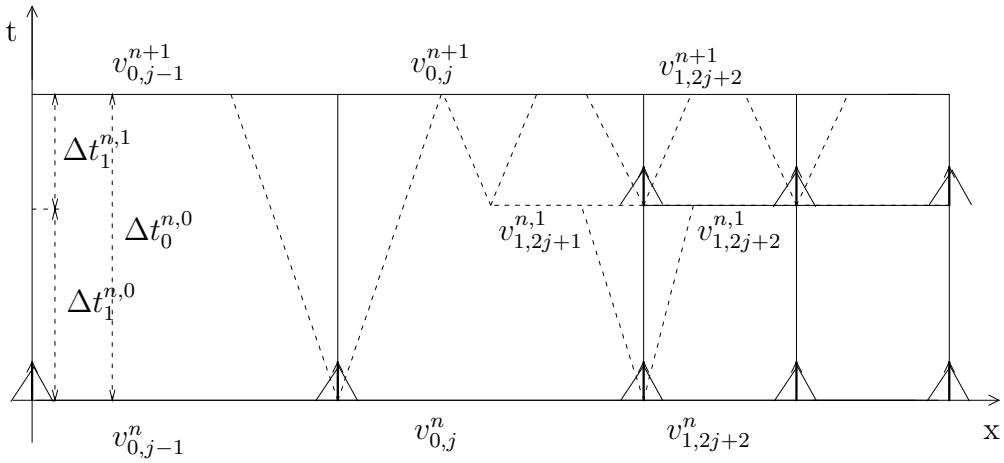

Figure 7: New scheme for the transition zone $\bar{C}_0$

We now show that the discrete solution computed using the specific steps (5.9)–(5.12) satisfies an entropy inequality at intermediate times $t^{n,i}$. At these time-steps, a partial regriding takes place, in which the thresholding and refinement operators are applied to the solution belonging to levels of discretization which have just been synchronized. The influence of these operators have already been studied in the previous section. The novelty with respect to the global time-step algorithm is the treatment of the transition zone for which we claim the following result.

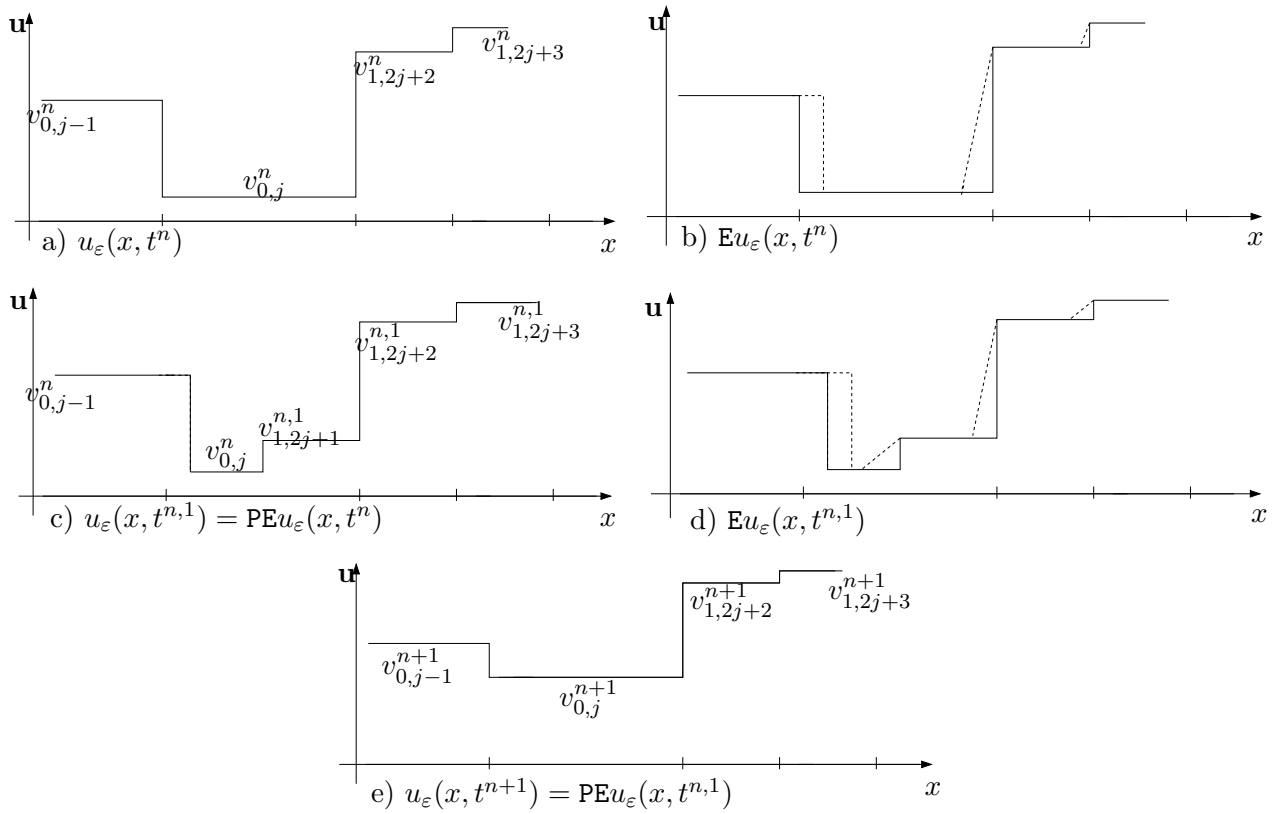

Figure 8: Evolution of the solution in the transition zone $\bar{C}_0 = \{\Omega_{0,j}\}$

Lemma 5.1. *Let (η, q) be an entropy/entropy-flux pair. Then, the discrete solution computed with Algorithms 8 and 9 satisfies*

$$\eta(v_{k,j}^{n,i+1}) - \eta(v_{k,j}^{n,i}) + \frac{\Delta t_k^{n,i}}{\Delta x_k}\big(\tilde{q}_{k,j+1}^{n,i} - \tilde{q}_{k,j}^{n,i}\big) \leq 0 \tag{5.13}$$

for $(k,j) \in \overline{\mathcal{C}}_k$ and for $i = 0, \ldots, 2^k - 1$, where the entropy fluxes are defined as

- *if $(k+1, 2j+2) \in \mathcal{C}_{k+1}$,*

$$\tilde{q}_{k,j}^{n,i} = q(\omega(0^+, v_{k,j-1}^{n,i}, v_{k,j}^{n,i})), \tag{5.14}$$
$$\tilde{q}_{k,j+1}^{n,i} = \frac{\Delta t_{k+1}^{n,2i}}{\Delta t_k^{n,i}} q(\omega(0^+, v_{k,j}^{n,i}, v_{k+1,2j+2}^{n,2i})) + \frac{\Delta t_{k+1}^{n,2i+1}}{\Delta t_k^{n,i}} q(\omega(0^+, v_{k+1,2j+1}^{n,2i+1}, v_{k+1,2j+2}^{n,2i+1}));$$

- *if $(k+1, 2j-1) \in \mathcal{C}_{k+1}$,*

$$\tilde{q}_{k,j}^{n,i} = \frac{\Delta t_{k+1}^{n,2i}}{\Delta t_k^{n,i}} q(\omega(0^+, v_{k+1,2j-1}^{n,2i}, v_{k,j}^{n,i})) + \frac{\Delta t_{k+1}^{n,2i+1}}{\Delta t_k^{n,i}} q(\omega(0^+, v_{k+1,2j-1}^{n,2i+1}, v_{k+1,2j}^{n,2i+1})),$$
$$\tilde{q}_{k,j+1}^{n,i} = q(\omega(0^+, v_{k,j}^{n,i}, v_{k,j+1}^{n,i})). \tag{5.15}$$

Proof. We detail the first case where the transition cell $\Omega_{k,j}$ is on the left-hand side of the finer level $k+1$. This corresponds to the two-level example depicted in Figure 8. We

write the entropy balance satisfied by the solution of the Cauchy problem on the cell $\Omega_{k,j}$ and study each intermediate time step separately. Integrating over the first time slab gives

$$\frac{1}{\Delta x_k}\int_{\Omega_{k,j}}\int_{t_{k+1}^{n,2i}}^{t_{k+1}^{n,2i+1}}\{\partial_t\eta(u_\varepsilon)+\partial_x q(u_\varepsilon)\}(x,t)dtdx=\frac{1}{\Delta x_k}\int_{\Omega_{k,j}}\eta(u_\varepsilon(x,t_{k+1}^{n,2i+1}))dx$$
$$-\eta(v_{k,j}^{n,i})+\frac{\Delta t_{k+1}^{n,2i}}{\Delta x_k}\big(q(\omega(0^+,v_{k,j}^{n,i}),v_{k+1,2j+2}^{n,2i})-q(\omega(0^+,v_{k,j-1}^{n,i},v_{k,j}^{n,i}))\big)\le 0. \tag{5.16}$$

We subdivide the cell $\Omega_{k,j}$ in the two sub-cells $\Omega_{k+1,2j}\cup\Omega_{k+1,2j+1}$, that is,

$$\frac{1}{\Delta x_k}\int_{\Omega_{k,j}}\eta(u_\varepsilon(x,t_{k+1}^{n,2i+1}))dx=\frac{1}{\Delta x_k}\int_{\Omega_{k+1,2j}}\dots+\frac{1}{\Delta x_k}\int_{\Omega_{k+1,2j+1}}\dots \tag{5.17}$$

By definition,

$$\frac{2}{\Delta x_k}\int_{\Omega_{k+1,2j+1}}u_\varepsilon(x,t_{k+1}^{n,2i+1})dx=v_{k+1,2j+1}^{n,2i+1}, \tag{5.18}$$

and since η is convex, we have

$$\eta(v_{k+1,2j+1}^{n,2i+1})\le\frac{2}{\Delta x_k}\int_{\Omega_{k+1,2j+1}}\eta(u_\varepsilon(x,t_{k+1}^{n,2i+1}))dx. \tag{5.19}$$

As a consequence, inequality (5.16) becomes

$$\frac{1}{\Delta x_k}\int_{\Omega_{k+1,2j}}\eta(u_\varepsilon(x,t_{k+1}^{n,2i+1}))dx+\frac{1}{2}\eta(v_{k+1,2j+1}^{n,2i+1})-\eta(v_{k,j}^{n,i}) \tag{5.20}$$
$$+\frac{\Delta t_{k+1}^{n,2i}}{\Delta x_k}\big(q(\omega(0^+,v_{k,j}^{n,i},v_{k+1,2j+2}^{n,2i}))-q(\omega(0^+,v_{k,j-1}^{n,i},v_{k,j}^{n,i}))\big)\le 0.$$

For the balance on the second intermediate time-step, we write

$$\frac{1}{\Delta x_k}\int_{\Omega_{k,j}}\eta(u_\varepsilon(x,t^{n,i+1}))dx-\frac{1}{\Delta x_k}\int_{\Omega_{k,j}}\eta(u_\varepsilon(x,t_{k+1}^{n,2i+1}))dx \tag{5.21}$$
$$+\frac{\Delta t_{k+1}^{n,2i+1}}{\Delta x_k}\big(q(\omega(0^+,v_{k+1,2j+1}^{n,2i+1},v_{k+1,2j+2}^{n,2i+1}))-q(\omega(0^+,v_{k,j-1}^{n,i},v_{k,j}^{n,i}))\big)\le 0.$$

By means of Jensen's inequality,

$$\eta(v_{k,j}^{n,i+1})\le\frac{1}{\Delta x_k}\int_{\Omega_{k,j}}\eta(u_\varepsilon(x,t^{n,i+1}))dx, \tag{5.22}$$

which transforms (5.21) into

$$\eta(v_{k,j}^{n,i+1})-\frac{1}{\Delta x_k}\int_{\Omega_{k,j}}\eta(u_\varepsilon(x,t_{k+1}^{n,2i+1}))dx \tag{5.23}$$
$$+\frac{\Delta t_{k+1}^{n,2i+1}}{\Delta x_k}\big(q(\omega(0^+,v_{k+1,2j+1}^{n,2i+1},v_{k+1,2j+2}^{n,2i+1}))-q(\omega(0^+,v_{k,j-1}^{n,i},v_{k,j}^{n,i}))\big)\le 0.$$

Adding (5.20) and (5.23) together, we end up with

$$\eta(v_{k,j}^{n,i+1})-\eta(v_{k,j}^{n,i})+\frac{1}{\Delta x_k}\big(\Delta t_{k+1}^{n,2i}q(\omega(0^+,v_{k,j}^{n,i},v_{k+1,2j+2}^{n,2i})) \tag{5.24}$$
$$+\Delta t_{k+1}^{n,2i+1}q(\omega(0^+,v_{k+1,2j+1}^{n,2i+1},v_{k+1,2j+2}^{n,2i+1}))-\Delta t_k^{n,i}q(\omega(0^+,v_{k,j-1}^{n,i},v_{k,j}^{n,i}))\big)\le 0,$$

which is none other than (5.13)–(5.14). □

5.2 Convergence of the scheme

Equipped with this result, we will now study the convergence of the LTS Algorithm 7, and we therefore design the numerical function solution $u_\varepsilon(x,t)$ analogous to (4.8b) solution of (2.1) on intervals $[t^{n,i}, t^{n,i+1}[$ and such that, for $i = 0, \dots, 2^K - 1$,

$$u_\varepsilon(x, t^{n,i}) = \begin{cases} v_{k,j}^{n,2^{k-K}i} & \text{if } x \in \Omega_{k,j},\ (k,j) \in \partial\widetilde{\Gamma}_\varepsilon^{n,i+1},\ k > k_i; \\ \bar{v}_{k_i,j}^{n,2^{k_i-K}i} & \text{if } x \in \Omega_{k_i,j},\ (k_i,j) \in \partial\widetilde{\Gamma}_\varepsilon^{n,i+1}; \\ \bar{v}_{k_i,2j+1}^{n,2^{k_i-K}i} & \text{if } x \in \Omega_{k_i,2j+1},\ (k_i-1,j) \in \bar{\mathcal{C}}_{k_i-1},\ (k_i,2j+2) \in \mathcal{C}_{k_i}; \\ \bar{v}_{k_i,2j}^{n,2^{k_i-K}i} & \text{if } x \in \Omega_{k_i,2j},\ (k_i-1,j) \in \bar{\mathcal{C}}_{k_i-1},\ (k_i,2j-1) \in \mathcal{C}_{k_i}; \\ u_\varepsilon(x, t^{n,i^-}) & \text{elsewhere.} \end{cases} \tag{5.25}$$

Algorithm 7 Synchronized time evolution for macro time step n

for each intermediate time step $i = 0, \dots, 2^K - 1$ **do**

• Initialization

for $k = K \searrow k_{i+1}$ **do**

update indices sets $\mathcal{C}_k$, $\overline{\mathcal{C}}_k$

end for

• Update fluxes at interfaces of cells that have been modified at previous time step on levels $k = K \searrow k_i$

• Time evolution

update solution in all cells in $\widetilde{S}_\varepsilon^{n,i+1}$ in levels $K \searrow k_{i+1}$

subdivide cells in $\overline{\mathcal{C}}_{k_{i+1}-1}$ (neighbors of $\mathcal{C}_{k_{i+1}}$) and update solution

• If i odd, perform thresholding `T` and regriding `R` on levels $k_{i+1}+1$ to K.

end for

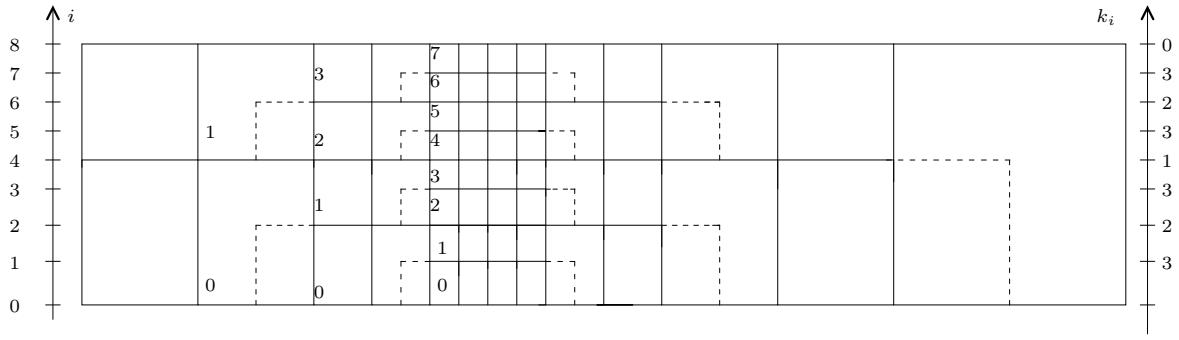

Figure 9: Multilevel local time stepping algorithm for $K = 3$. The intermediate time steps $i = 0, \dots, 8$ are denoted on the left vertical axis. The corresponding synchronization level is denoted on the right vertical axis

The Local Time Stepping numerical scheme is studied as a succession of four operators applied on $u_\varepsilon(x, t^{n,i})$, namely:

- Operator `E` (Evolution): compute the solution of the Cauchy problem (2.1-5.25) on the time step $[t^{n,i}, t^{n,i+1}[$ on all cells $\Omega_{k,j}$, $(k,j) \in \partial\widetilde{\Gamma}_\varepsilon^{n,i+1}$, $k \geq k_{i+1}$. Leave the solution unchanged elsewhere. We use the notation

$$\mathtt{E}u_\varepsilon(x, t^{n,i}) = u_\varepsilon(x, t^{n,i+1;-}). \tag{5.26}$$

Algorithm 8 Updating of fluxes at intermediate time step i

• Update fluxes on left edge cells that have been modified at the previous time step :
initialize $m = i$
for levels $k = K \searrow k_i$ **do**
  for $(k,j) \in \partial\widetilde{\Gamma}_\varepsilon^{n,i+1}$ **do**
    compute $\hat{f}_{k,j}^{n,m} = \hat{F}(v_{k,j-1}^{n,m}, v_{k,j}^{n,m})$
  end for
  $m = m/2$
end for
compute $\Delta t^{n,i}$ satisfying the CFL stability condition (5.5)
• Update fluxes on neighbors of $\mathcal{C}_{k_i}$
for $(k,j) \in \overline{\mathcal{C}}_{k_i-1}$ **do**
  if $(k+1, 2j-1) \in \partial\widetilde{\Gamma}_\varepsilon^{n,i+1}$ **then**
    compute $\hat{f}_{k_i,2j}^{n,2m} = \hat{F}(v_{k_i,2j-1}^{n,2m}, v_{k_i,2j}^{n,2m})$
    update $\hat{f}_{k,j}^{n,m} = \frac{\Delta t_{k+1}^{n,2m}}{\Delta t_k^{n,m}} \hat{f}_{k,j}^{n,m} + \frac{\Delta t_{k+1}^{n,2m+1}}{\Delta t_k^{n,m}} \hat{f}_{k+1,2j}^{n,2m+1}$
  else if $(k+1, 2j+2) \in \partial\widetilde{\Gamma}_\varepsilon^{n,i+1}$ **then**
    update $\hat{f}_{k,j+1}^{n,m} = \frac{\Delta t_{k+1}^{n,2m}}{\Delta t_k^{n,m}} \hat{f}_{k+1,2j+2}^{n,2m} + \frac{\Delta t_{k+1}^{n,2m+1}}{\Delta t_k^{n,m}} \hat{f}_{k+1,2j+2}^{n,2m+1}$
  end if
end for

- Operator P (Projection):
  - Compute the average of the Cauchy problem solution on the cells of the grid $\widetilde{S}_\varepsilon^{n+1}$ on levels finer than the synchronization level.
  - Apply the special procedure on transition zone cells.
  - Leave the solution unchanged in all other cells.

  We denote by $\bar{v}_{k,j}^{\varepsilon,n,i+1}$ the discrete values such that

$$\mathtt{P}u_\varepsilon(x, t^{n,i+1;-}) = \bar{v}_{k,j}^{n,2^{k-K}(i+1)} \quad \text{for } x \in \Omega_{k,j},\ (k,j) \in \partial\widetilde{\Gamma}_\varepsilon^{n,i+1},\ k \geq k_{i+1}. \tag{5.27}$$

  In the transition zone, setting $k = k_{i+1} - 1$, we have

  - for cells $(k,j) \in \bar{\mathcal{C}}_k$ such that $(k+1, 2j-1) \in \tilde{\mathcal{I}}_{k_{i+1}}$,

$$\mathtt{P}u_\varepsilon(x, t^{n,i+1;-}) = \begin{cases} \bar{v}_{k_{i+1},2j}^{n,2^{k_{i+1}-K}(i+1)} & \text{for } x \in \Omega_{k_{i+1},2j}, \\ u_\varepsilon(x, t^{n,i+1;-}) & \text{elsewhere;} \end{cases} \tag{5.28}$$

  - for cells $(k,j) \in \bar{\mathcal{C}}_k$ such that $(k+1, 2j+2) \in \tilde{\mathcal{I}}_{k_{i+1}}$,

$$\mathtt{P}u_\varepsilon(x, t^{n,i+1;-}) = \begin{cases} \bar{v}_{k_{i+1},2j+1}^{n,2^{k_{i+1}-K}(i+1)} & \text{for } x \in \Omega_{k_{i+1},2j+1}, \\ u_\varepsilon(x, t^{n,i+1;-}) & \text{elsewhere.} \end{cases} \tag{5.29}$$

  At the discrete level, the values $\bar{v}_{k,j}^{n,2^{k-K}(i+1)}$ are computed using the Algorithms 8 and 9. The evolution and projection are performed together, only on cells in level $k \geq k_{i+1}$ or in the transition zone. However, to simplify the proofs, it is useful to consider that the Evolution E is performed everywhere at each intermediate time-step, so that the numerical solution u_ε is defined everywhere.

Algorithm 9 Updating of solution at intermediate time step i

initialize $m = i$
for levels $k = K \searrow k_{i+1}$ **do**
  for $(k,j) \in \partial\widetilde{\Gamma}_\varepsilon^{n,i}$ **do**
    $\bar{v}_{k,j}^{n,m+1} = \bar{v}_{k,j}^{n,m} - \frac{\Delta t_k^{n,m}}{\Delta x_k}\big(\hat{f}_{k,j}^{n,m} - \hat{f}_{k,j-1}^{n,m}\big)$,
  end for
  $m = m/2$
end for
for $(k,j) \in \overline{\mathcal{C}}_{k_{i+1}-1}$ **do**
  if $(k+1, 2j+2) \in \mathcal{C}_{k_{i+1}}$ **then**
    subdivide cell $\Omega_{k,j}$ and update solution on cell $\Omega_{k+1,2j+1}$
    $\bar{v}_{k+1,2j+1}^{n,2m+1} = \bar{v}_{k,j}^{n,m} - \frac{\Delta t_{k+1}^{n,2m}}{\Delta x_{k+1}}\big(\hat{f}_{k+1,2j+2}^{n,2m} - f(v_{k,j}^{n,m})\big)$
  else if $(k+1, 2j-1) \in \mathcal{C}_{k_{i+1}}$ **then**
    subdivide cell $\Omega_{k,j}$ and update solution on cell $\Omega_{k+1,2j}$:
    $\bar{v}_{k+1,2j}^{n,2m+1} = \bar{v}_{k,j}^{n,m} - \frac{\Delta t_{k+1}^{n,2m}}{\Delta x_{k+1}}\big(f(v_{k,j}^{n,m}) - \hat{f}_{k+1,2j}^{n,2m}\big)$
  end if
end for

- Operator `T` (Thresholding):
  - Encode the solution $(\bar{v}_{k,j}^{n,2^{k-K}(i+1)})_{k,j}$ for $(k,j) \in \partial\widetilde{\Gamma}_\varepsilon^{n,i+1}$, $k > k_{i+1}$.
  - Apply the multiresolution thresholding to design $\Gamma_\varepsilon^{n,i+1}$
  - Decode/coarsen the solution on the grid $S_\varepsilon^{n,i+1} = S(\Gamma_\varepsilon^{n,i+1})$, for levels $k > k_{i+1}$.

  We denote by $\check{v}_{k,j}^{n,2^{k-K}(i+1)}$ the discrete values such that

$$\mathtt{TP}u_\varepsilon(x, t^{n,i+1;-}) = \begin{cases} \check{v}_{k,j}^{n,2^{k-K}(i+1)} & \text{for } x \in \Omega_{k,j},\ \ (k,j) \in \partial\Gamma_\varepsilon^{n,i+1},\ \ k > k_{i+1}, \\ \mathtt{P}u_\varepsilon(x, t^{n,i+1;-}) & \text{elsewhere.} \end{cases} \tag{5.30}$$

- Operator `R` (Refinement):
  - Predict the tree $\tilde{\Gamma}_\varepsilon^{n,i+2}$ containing both $\Gamma_\varepsilon^{n,i+1}$ and $\Gamma_\varepsilon^{n,i+2}$ using Algorithm 5, for levels $k > k_{i+1}$.
  - Set to 0 the details $d_{k,j}$ for $(k,j) \in \Gamma_\varepsilon^{n,i+2}$ and $(k,j) \notin \Gamma_\varepsilon^{n,i+1}$.
  - Refine the solution from $S_\varepsilon^{n,i+1}$ to $\tilde{S}_\varepsilon^{n,i+2} = S(\tilde{\Gamma}_\varepsilon^{n,i+2})$ using the partial refinement algorithm 2.

  We are back to the values on the predicted grid $\tilde{S}_\varepsilon^{n,i+2}$ such that

$$\mathtt{RTP}u_\varepsilon(x, t^{n,i+1;-}) = u_\varepsilon(x, t^{n,i+1}),\ \ \text{for } x \in \Omega_{k,j},\ \ (k,j) \in \partial\widetilde{\Gamma}_\varepsilon^{n+2}, \tag{5.31}$$

  with $u_\varepsilon(x, t^{n,i+1})$ defined by (5.25). Note that the thresholding and refinement operations occur only at the end of odd intermediate time-steps since $k_{i+1} = K$ for even values of i.

The convergence of this numerical solution towards the weak entropy solution of (2.1) is ensured by the following results, which can be considered as counterparts of Proposition 4.2 and Theorem 4.1.

Proposition 5.1. *Consider the Cauchy problem (2.1) with $u_0 \in L^\infty(\mathbb{R}_x)$. For any given fixed time $T > 0$, discretized as*

$$T = \sum_{n=0}^{N} \sum_{i=0}^{2^K-1} \Delta t^{n,i}, \tag{5.32}$$

let us consider the CFL restriction

$$\frac{\Delta t^{n,i}}{2^{-K}\Delta x} \max_{|u|\leq C(T)} |f'(u)| \leq \frac{1}{3}, \tag{5.33}$$

where $C(T)$ is defined by (4.40), and let ε satisfy (4.37). Then, the sequence of numerical solutions $(u_\varepsilon)_{\varepsilon\geq 0}$ computed by the method (5.25)–(5.30) is uniformly bounded in $L^\infty([0,T[\times\mathbb{R}_x)$ with

$$\|u_\varepsilon\|_{L^\infty(]0,T[\times\mathbb{R}_x)} \leq C(T). \tag{5.34}$$

Note that contrary to the uniform time-step used in the previous section, the time interval $[0,T]$ where the solution is studied is discretized using time-steps $\Delta t_k^{n,i}$ as described in (5.1)–(5.4), so that in the end T is given by (5.32).

Theorem 5.1. *Consider the Cauchy problem (2.1) with $u_0 \in L^\infty(\mathbb{R}_x)$. Let $(u_\varepsilon)_{\varepsilon\geq 0}$ be the sequence of approximate solutions computed by the method (5.25)–(5.30). Assume that the discretization parameters ε, $\Delta t^{n,i}$, and Δx are such that for any given fixed time $T > 0$, there exists a constant $C_T > 0$, independent of the discretization coefficients, such that*

$$\frac{\Delta x}{\Delta t^{n,i}} + \frac{\varepsilon}{\Delta t^{n,i}} \leq C_T. \tag{5.35}$$

Then, the sequence $(u_\varepsilon)_{\varepsilon\geq 0}$ converges strongly in $L^1_{loc}(]0,T[\times\mathbb{R}_x)$ to the unique entropy weak solution u of (2.1) under the CFL condition (5.33). In other words, for any given time $T > 0$ and any compact $B \subset \mathbb{R}_x$, we have

$$\|u_\varepsilon - u\|_{L^1(]0,T[\times B)} \leq r(\varepsilon), \tag{5.36}$$

where $r(\varepsilon)$ tends to zero in the limit $\varepsilon \to 0$.

The proofs of Proposition 5.1 and Theorem 5.1 rely on intermediate results similar to Lemmas 4.3, 4.4, 4.5 and 4.6. Before stating the new Lemmas and sketching out their proofs, let us again emphasize that between intermediate time steps $t^{n,i}$ and $t^{n,i+1}$, only the solution defined on cells on levels $k \geq k_{i+1}$ is modified, where k_i is the synchronization level defined by (5.6).

The counterpart of Lemma 4.3 is

Lemma 5.2. *For any non-negative test function $\phi \in \mathscr{C}_c^1(\mathbb{R}_t^+ \times \mathbb{R}_x)$ and for any given entropy/entropy-flux pair (η, q), the entropy weak inequality*

$$\begin{aligned}\int_{\mathbb{R}_x} \eta(u_\varepsilon(x,T))\phi(x,T)dx - \int_{\mathbb{R}_x} \eta(u_\varepsilon^0(x))\phi(x,0)dx - \int_0^T \int_{\mathbb{R}_x} \big\{\eta(u_\varepsilon)\partial_t\phi + q(u_\varepsilon)\partial_x\phi\big\}(x,t)dxdt \\ \leq \sum_{n=0}^{N} \sum_{i=0}^{2^K-1} \int_{\mathbb{R}_x} \big[\eta(\mathtt{RTPE}u_\varepsilon) - \eta(\mathtt{E}u_\varepsilon)\big](x,t^{n,i})\phi(x,t^{n,i+1})dx\end{aligned} \tag{5.37}$$

holds under the CFL restriction (5.33).

The counterpart of Lemma 4.4 is

Lemma 5.3. *For any test function $\phi \in \mathscr{C}_c^1(\mathbb{R}_t^+ \times \mathbb{R}_x)$ and for any smooth function η, the estimate*

$$\sum_{n=0}^{N} \sum_{i=0}^{2^K-1} \int_{\mathbb{R}_x} \big[\eta(\mathtt{RTPE}u_\varepsilon) - \eta(\mathtt{TPE}u_\varepsilon)\big](x, t^{n,i}) \phi(x, t^{n,i+1}) dx \leq C\varepsilon \|\phi\|_{L^\infty(\mathbb{R}_t^+, W^{1,\infty}(\mathbb{R}_x))} \quad (5.38)$$

holds under assumption (5.35) of Theorem 5.1, where $C > 0$ is some uniform constant.

Finally, the counterpart of Lemma 4.5 is

Lemma 5.4. *For any nonnegative test function $\phi \in \mathscr{C}_c^1(\mathbb{R}_t^+ \times \mathbb{R}_x)$ and for any smooth convex function η, the estimate*

$$\sum_{n=0}^{N} \sum_{i=0}^{2^K-1} \int_{\mathbb{R}_x} \big[\eta(\mathtt{TPE}u_\varepsilon) - \eta(\mathtt{E}u_\varepsilon)\big](x, t^{n,i}) \phi(x, t^{n,i+1}) dx \leq C\varepsilon^{1/2} \|\phi\|_{L^\infty(\mathbb{R}_t^+, W^{1,\infty}(\mathbb{R}_x))} \quad (5.39)$$

holds under the CFL condition (5.33), where $C > 0$ is some uniform constant.

The proof of Lemma 5.4 relies on the following weak BV-like estimate analogous to the one stated in lemma 4.6.

Lemma 5.5. *Let $T > 0$ be any given fixed time and let B be any given compact interval of $\mathbb{R}_x$. Then, under the CFL condition (5.33), there exists a positive constant C independent of ε such that*

$$\sum_{n=0}^{N} \sum_{i=0}^{2^K-1} \int_{B} |\mathtt{E}u_\varepsilon - \mathtt{TPE}u_\varepsilon|^2(x, t^{n,i}) dx \leq C. \quad (5.40)$$

Proofs of the Lemmas. The proofs of Lemmas 5.2, 5.3, 5.4 and 5.5 follow very closely the steps of their counterparts in section 4.2. The only technical difficulty is that all time integrals must now be split over time-steps $t^{n,i}$, with

$$n \in \{0, 1, \ldots, T/\Delta t - 1\} \quad \text{and} \quad i \in \{0, 1, \ldots, 2^K - 1\}.$$

Likewise, all space integrals must now be split over cells $\Omega_{k,i}$ with $(k, j) \in \partial\Gamma_\varepsilon^{n,i+1}$. Furthermore, the discrete test function must be redefined as (see (5.30))

$$\phi_\varepsilon(x, t^{n,i}) \equiv \phi_{k,j}^{n,i} = \frac{1}{\Delta x_k} \int_{\Omega_{k,j}} \phi(x, t^{n,i}) dx, \qquad x \in \Omega_{k,j}, \ \ (k, j) \in \partial\Gamma_\varepsilon^{n,i+1}. \quad (5.41)$$

In the proof of Lemma 5.3, for instance, mimicking the proof of Lemma 4.4 we begin with the identity

$$\begin{aligned} \int_{\mathbb{R}_x} \big[\eta(\mathtt{RTPE}u_\varepsilon) - \eta(\mathtt{TPE}u_\varepsilon)\big](x, t^{n,i}) \phi(x, t^{n,i+1}) dx \\ = \int_{\mathbb{R}_x} \big[\eta(\mathtt{RTPE}u_\varepsilon) - \eta(\mathtt{TPE}u_\varepsilon)\big](x, t^{n,i}) \big[\phi - \phi_\varepsilon\big](x, t^{n,i+1}) dx \\ + \sum_{(k,j) \in \partial\Gamma_\varepsilon^{n,i+1}} \phi_{k,j}^{n,i+1} \int_{\Omega_{k,j}} \big[\eta(\mathtt{RTPE}u_\varepsilon) - \eta(\mathtt{TPE}u_\varepsilon)\big](x, t^{n,i}) dx. \end{aligned} \quad (5.42)$$

At this point the integral on $\mathbb{R}_x$ is split over integrals on cells $\Omega_{k,j}$ with $(k,j) \in \partial\Gamma_\varepsilon^{n,i+1}$. Thanks to (5.30), on cells $\Omega_{k,j}$ with $k \leq k_{i+1}$, nothing is done. Therefore,

$$\eta(\mathtt{RTPE}u_\varepsilon(x,t^{n,i})) = \eta(\mathtt{TPE}u_\varepsilon(x,t^{n,i})) = \eta(\mathtt{E}u_\varepsilon(x,t^{n,i})). \tag{5.43}$$

This means in particular that the thresholding and reconstruction are performed only at odd intermediate time-steps (since $k_{i+1} = K$ otherwise). Wherever and whenever something must be done, that is, on cells belonging to levels above the synchronization level k_{i+1}, the norm $\|\{\eta(\mathtt{RTPE}u_\varepsilon) - \eta(\mathtt{TPE}u_\varepsilon)\}(.,t^{n,i})\|_{L^\infty}$ is bounded thanks to (4.34). □

6 Numerical application

This section is devoted to the numerical illustration of the theoretical convergence behavior obtained in sections 4 and 5. We apply the adaptive multiresolution scheme to the Burgers equation, i.e., with $f(u) = u^2/2$. Two distinct initial conditions are considered: (i) a smooth one

$$u_0^s(x) = e^{-50(x-0.5)^2} \tag{6.1}$$

and (ii) a discontinuous one inspired from [26]

$$u_0^d(x) = \begin{cases} 3 & \text{if } x < 0.1 \\ -2 & \text{if } 0.1 \leq x < 0.5 \\ 5 & \text{if } 0.5 \leq x < 0.9 \\ -5 & \text{otherwise.} \end{cases} \tag{6.2}$$

Simulations are performed on the unit space interval $x \in [0,1]$ with Neumann boundary conditions. Several discretizations and threshold levels are used.

In Figure 10, we display the results for the smooth initial condition at the end time $T = 0.05$s at which the exact solution is still smooth. It can therefore be computed by the characteristic method. We compute the relative L^1-error

$$\mathcal{E}_{L^1} = \frac{\displaystyle\sum_{j=0}^{N_0 2^K - 1} |v_{K,j} - v_{K,j}^{\text{exact}}|}{\displaystyle\sum_{j=0}^{N_0 2^K - 1} |v_{K,j}^{\text{exact}}|} \tag{6.3}$$

between the numerical solution and the exact solution, where $v_{K,j}$ is the adaptive solution reconstructed on the finest level K using Algorithm 2 and $v_{K,j}^{\text{exact}}$ is the mean value of the exact solution on cell $\Omega_{K,j}$. We refer to Remark 3.1 for the definition of the spatial index N_0 such that $L = N_0 \Delta x_0$. The curves corresponding to 3 different discretizations are displayed, in all cases for a 8-level multiresolution hierarchy and starting with 2, 4 and 8 cells on the coarsest level. For each discretization, the L^1-error is plotted against the threshold parameter ε, which is sampled on 15 different values. The horizontal line correspond to the discretization error, that is to the L^1-error between the discrete and the exact solution obtained on the uniform finest grid (512, 1024 or 2048 cells).

The simulations confirm that when the threshold ε goes to zero, the error between the adaptive and the exact solution tends to the discretization error. This is the normally

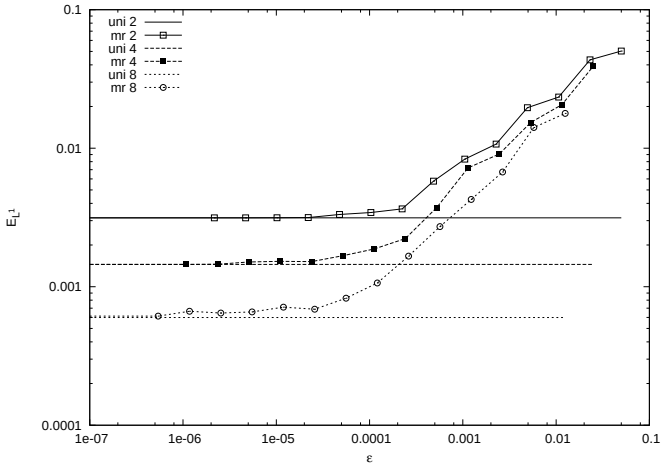

Figure 10: Relative L_1-error between numerical and exact solution for the smooth initial condition (6.1). Multiresolution on 8 levels. 2, 4 and 8 cells on the coarsest level

expected behavior, since the error due to the multiresolution goes to zero according to (3.17a). The same experiment is performed for the discontinuous initial condition (6.2) and displayed in Figure 11. We then use these curves and other results not represented here corresponding to finer discretizations ($N_0 = 16$, 32, 64, and 128) to validate the hypothesis on the relation (4.37) between ε and Δx_0. Recall that the ratio $\Delta t_0/\Delta x_0$ is fixed. For each discretization, we graphically estimate the value of ε corresponding to a multiresolution error equal to the discretization error and we plot this value as a function of Δx_0 in Figure 12. For both initial condition an asymptotic behavior is observed, in $\Delta x_0^{1.1}$ in the smooth case and $\Delta x_0^{1.01}$ in the discontinuous case. These results therefore validate our assumption (4.37).

A Main results for Young measures

We recall here the main definitions and results used in the Coquel-LeFloch methodology [10].

First, we need to define measure-valued solutions which extend the notion of weak solution. Instead of functions in $L^\infty(\mathbb{R}\times]0,T[)$, we consider Young measures on $\mathbb{R}\times]0,T[$ that are weak-$\star$ bounded applications

$$\nu : \mathbb{R}\times]0,T[\longrightarrow \nu_{x,t} \in \mathrm{Prob}(\mathbb{R})$$

such that for all functions $a \in \mathscr{C}(\mathbb{R};\mathbb{R})$

$$\langle \nu_{x,t}, a\rangle = \int_{\mathbb{R}} a(\lambda) d\nu_{x,t}(\lambda), \quad \text{a.e. } (x,t) \in \mathbb{R}\times]0,T[$$

Weak-$\star$ boundedness means that $(x,t) \mapsto \langle \nu_{x,t}, a\rangle$ is in $L^\infty(\mathbb{R}\times]0,T[)$. Moreover, it is assumed that all measures under consideration are supported in a compact set $K \subset \mathbb{R}$, that is,

$$\langle \nu_{x,t}, a\rangle = 0 \tag{A.1}$$

for all continuous functions a vanishing on K.

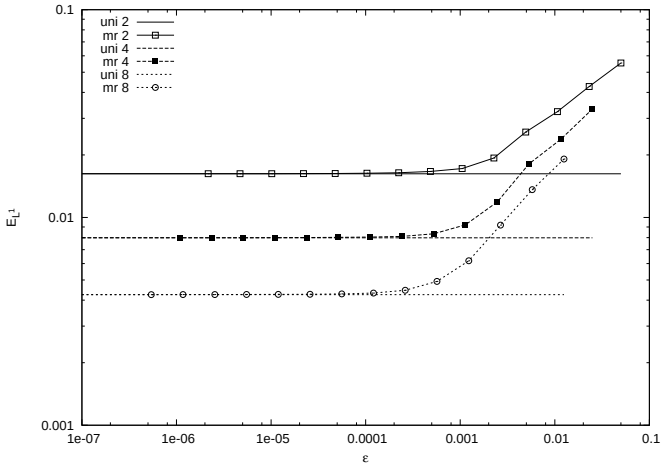

Figure 11: Relative L_1-error between numerical and exact solution for the discontinuous initial condition (6.2). Multiresolution on 8 levels. 2, 4 and 8 cells on the coarsest level

Definition A.1. *A Young measure $\nu : \mathbb{R}\times]0,T[\longrightarrow Prob(\mathbb{R})$ is a measure-valued solution of (2.1) if it satisfies*

$$\partial_t\langle\nu, Id\rangle + \partial_x\langle\nu, f\rangle = 0 \tag{A.2}$$

in the usual sense of distributions.

We remark that if $u \in L^\infty(\mathbb{R}\times]0,T[)$ is a weak solution of (2.1), then the Young measure defined by

$$\nu_{x,t} = \delta_{u(x,t)} \tag{A.3}$$

is a measure-valued solution of (2.1). As in the weak sense, an entropy condition is necessary to ensure uniqueness of a measure-valued solution.

Definition A.2. *A Young measure ν is consistent with the entropy inequality (2.2) associated with (η, q) if it satisfies*

$$\partial_t\langle\nu_{x,t}, \eta\rangle + \partial_x\langle\nu_{x,t}, q\rangle \leq 0 \tag{A.4}$$

in the sense of distributions. A measure-valued solution ν is an entropy measure-valued solution if it satisfies (A.4) for all entropy/entropy-flux pair (η, q).

By extension of Kruzkov's uniqueness result [17], DiPerna's theorem asserts that an entropy measure-valued solution is unique in L^∞.

Theorem A.1. *(DiPerna). Let $u_0 \in L^\infty(\mathbb{R})$. Suppose that $\nu : \mathbb{R}\times]0,T[\longrightarrow Prob(\mathbb{R})$ is a Young measure satisfying*

1. *ν is a measure-valued solution of (2.1),*
2. *ν is consistent with all the entropy inequalities (A.4),*
3. *for all compact set K in $\mathbb{R}$*

$$\lim_{\substack{t\to 0\\ t>0}} \int_0^t \int_K \langle\nu_{x,s}, |Id - u_0(x)|\rangle\, dxds = 0. \tag{A.5}$$

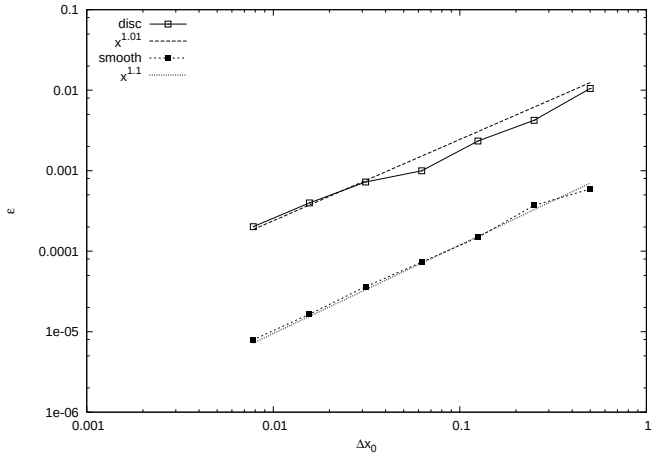

Figure 12: Value of threshold ε for which the multiresolution error is of the order of the discretization error

If $u \in L^\infty(\mathbb{R}\times]0,T[)$ is the unique weak entropy solution of (2.1), then

$$\nu_{x,t} = \delta_{u(x,t)}, \quad a.e.\ (x,t) \in \mathbb{R}\times]0,T[\tag{A.6}$$

The following theorem provides a sufficient condition to ensure condition (A.5) of Theorem A.1

Theorem A.2. *(DiPerna [13]). Let $u_0 \in L^\infty(\mathbb{R})$. Suppose that $\nu : \mathbb{R}\times]0,T[\longrightarrow Prob(\mathbb{R})$ is a Young measure assuming u_0 in the weak sense, i.e., for all $\varphi \in \mathscr{C}_0^1(\mathbb{R};\mathbb{R})$,*

$$\lim_{\substack{t\to 0\\ t>0}} \frac{1}{t}\int_0^t \int_{\mathbb{R}} \langle \nu_{x,s}, Id\rangle \varphi(x)dxds = \int_{\mathbb{R}} u_0(x)\varphi(x)dx. \tag{A.7}$$

Furthermore, assume that for all $\varphi \in \mathscr{C}_0^1(\mathbb{R};\mathbb{R}) \geq 0$ and for at least one continuous strictly convex function $\eta : \mathbb{R} \to \mathbb{R}$,

$$\lim_{t>0} \frac{1}{t}\int_0^t \int_{\mathbb{R}} \langle \nu_{x,s}, \eta\rangle \varphi(x)dxds \leq \int_{\mathbb{R}} \eta(u_0(x))\varphi(x)dx. \tag{A.8}$$

Then, ν assumes the initial condition in L^1_{loc} strongly (condition A.5 of Theorem A.1).

References

[1] N. Andrianov, F. Coquel, M. Postel, and Q. H. Tran. A linearly semi-implicit AMR method for 1-D gas-liquid flows. In A. A. Mammoli and C. A. Brebbia, editors, *Proceedings of the 3rd International Conference on Computational Methods in Multiphase Flow, Portland, Maine, October 2005*, number III in Computational Methods in Multiphase Flows, pages 295–304, Berlin, 2005. WIT Press.

[2] N. Andrianov, F. Coquel, M. Postel, and Q. H. Tran. A relaxation multiresolution scheme for accelerating realistic two-phase flows calculations in pipelines. *Int. J. Numer. Meth. Fluids*, 54(2):207–236, 2006.

[3] Marsha J. Berger and Joseph Oliger. Adaptive mesh refinement for hyperbolic partial differential equations. *J. Comput. Phys.*, 53(3):484–512, 1984.

[4] F. Bramkamp, P. Lamby, and S. Müller. An adaptive multiscale finite volume solver for unsteady and steady state flow computations. *J. Comput. Phys.*, 197(2):460–490, 2004.

[5] A. Cohen. Wavelet methods in numerical analysis. In P. G. Ciarlet and J. L. Lions, editors, *Handbook of Numerical Analysis*, volume VII, pages 417–711. Elsevier, North-Holland, 2000.

[6] A. Cohen, S. M. Kaber, S. Müller, and M. Postel. Fully adaptive multiresolution finite volume schemes for conservation laws. *Math. Comp.*, 72(241):183–225, 2003.

[7] F. Coquel, Q. L. Nguyen, M. Postel, and Q. H. Tran. Local time stepping applied to implicit-explicit methods for hyperbolic systems. *Multiscale Model. Simul.*, 8(2):540–570, 2010.

[8] F. Coquel, M. Postel, N. Poussineau, and Q. H. Tran. Multiresolution technique and explicit-implicit scheme for multicomponent flows. *J. Numer. Math.*, 14(3):187–216, 2006.

[9] Frédéric Coquel and Philippe LeFloch. Convergence of finite difference schemes for conservation laws in several space variables: the corrected antidiffusive flux approach. *Math. Comp.*, 57(195):169–210, 1991.

[10] Frédéric Coquel and Philippe LeFloch. Convergence of finite difference schemes for conservation laws in several space dimensions: a general theory. *SIAM J. Numer. Anal.*, 30(3):675–700, 1993.

[11] C[onstantine] M. Dafermos. *Hyperbolic Conservation Laws in Continuum Physics*, volume 325 of *Grundlehren der mathematischen Wissenschaften*. Springer-Verlag, Berlin, 2000.

[12] Ronald J. DiPerna. Convergence of approximate solutions to conservation laws. *Arch. Rational Mech. Anal.*, 82(1):27–70, 1983.

[13] Ronald J. DiPerna. Measure-valued solutions to conservation laws. *Arch. Rational Mech. Anal.*, 88(3):223–270, 1985.

[14] Margarete O. Domingues, Sônia M. Gomes, Olivier Roussel, and Kai Schneider. An adaptive multiresolution scheme with local time stepping for evolutionary PDEs. *J. Comput. Phys.*, 227(8):3758–3780, 2008.

[15] R. Eymard, T. Gallouët, and R. Herbin. Finite-volume methods. In P. G. Ciarlet et J. L. Lions, editor, *Handbook of Numerical Analysis*, volume 7, pages 715–1022. Elsevier, Amsterdam, 2000.

[16] E[dwige] Godlewski and P[ierre] A[rnaud] Raviart. *Hyperbolic Systems of Conservation Laws*, volume 3/4 of *Mathématiques et Applications, Société de Mathématiques Appliquées et Industrielles*. Ellipses, Paris, 1991.

[17] E[dwige] Godlewski and P[ierre] A[rnaud] Raviart. *Numerical approximation of hyperbolic systems of conservation laws*, volume 118 of *Applied Mathematical Sciences*. Springer, New-York, 1996.

[18] A. Harten. High resolution schemes for hyperbolic conservation laws. *J. Comput. Phys.*, 49:357–393, 1983.

[19] A. Harten. Multiresolution algorithms for the numerical solutions of hyperbolic conservation laws. *Comm. Pure Appl. Math.*, 48(12):1305–1342, 1995.

[20] N. Hovhannisyan and S. Müller. On the stability of fully adaptive multiscale schemes for conservation laws using approximate flux and source reconstruction strategies. *IMA J. Numer. Anal.*, 30(4):1256–1295, 2010.

[21] S. N. Kruzkov. First-order quasilinear equations in several independent variables. *Mat. USSR Sb.*, 10(2):217–243, 1970.

[22] P. Lamby, S. Müller, and Y. Stiriba. Solution of shallow water equations using fully adaptive multiscale schemes. *Int. J. Numer. Meth. Fluids*, 49(4):417–437, 2005.

[23] A. Y. Leroux and P. Quesseveur. Convergence of an antidiffusion Lagrange-Euler scheme for quasilinear equations. *SIAM J. Numer. Anal.*, 21(5):985–994, 1984.

[24] Y. G. Lu. *Hyperbolic Conservation Laws and the Compensated Compactness Method*, volume 128 of *Monographs and Surveys in Pure and Applied Mathematics*. Chapman & Hall/CRC, Boca Raton, 2003.

[25] S. Müller, P. Helluy, and J. Ballmann. Numerical simulation of a single bubble by compressible two-phase fluids. *Int. J. Numer. Meth. Fluids*, 62(6):591–631, 2010.

[26] S. Müller and Y. Stiriba. Fully adaptive multiscale schemes for conservation laws employing locally varying time stepping. *J. Sci. Comput.*, 30(3):493–531, 2007.

[27] S. Müller and Y. Stiriba. A multilevel finite-volume method with multiscale-based grid adaptation for steady compressible flows. *J. Comput. Appl. Math.*, 227(2):223–233, 2009. Special Issue on Emergent Applications of Fractals and Wavelets in Biology and Biomedicine.

[28] François Murat. Compacité par compensation. *Ann. Scuola Norm. Sup. Pisa Cl. Sci. Fis.*, 5(3):489–507, 1978.

[29] S. Osher and R. Sanders. Numerical approximations to nonlinear conservation laws with locally varying time and space grids. *Math. Comp.*, 41(164):321–336, 1983.

[30] O. Roussel, K. Schneider, A. Tsigulin, and H. Bockhorn. A conservative fully adaptive multiresolution algorithm for parabolic PDEs. *J. Comput. Phys.*, 188(2):493–523, 2003.

[31] C. W. Shu. TVB uniformly high order schemes for conservation laws. *Math. Comp.*, 49(179):105–121, 1987.

[32] J[oel] Smoller. *Shock Waves and Reaction-Diffusion Equations*, volume 258 of *Grundlehren der mathematischen Wissenschaften*. Springer-Verlag, New York, 1994.

[33] A. Szepessy. Convergence of a shock-capturing streamline diffusion finite element method for a scalar conservation law in two space dimensions. *Math. Comp.*, 53(188):527–545, 1989.

[34] L. Tartar. Compensated compactness and applications to partial differential equations. In R. J. Knops, editor, *Nonlinear analysis and mechanics: Heriot-Watt Symposium IV*, volume 39 of *Research Notes in Mathematics*, pages 136–212. Pitman, Boston, 1979.

[35] A. I. Vol'pert. The BV space and quasilinear equations. *Math. USSR Sb.*, 2:257–267, 1967.